Overexpression of human acid ceramidase precursor and variants of the catalytic center in Sf9 cells

Analysis of ceramidase maturation , autocatalytic processing and interaction with Sap-D

Dissertation
zur
Erlangung des Doktorgrades
der
Mathematisch-Naturwissenschaftlichen Fakultät
der
Rheinischen Friedrich-Wilhelms-Universität Bonn

vorgelegt von
Chih-Te Chien
aus Taiwan

Bonn 2009

Angefertigt mit Genehmigung der Mathematisch-Naturwissenschaftlichen Fakultät der Rheinischen Friedrich-Wilhelms-Universität Bonn.

Diese Dissertation ist auf dem Hochschulschriftenserver der ULB Bonn http://hss.ulb.unibonn.de/diss_online elektronisch publiziert. Erscheinungsjahr 2009

1. Referent: Prof. Dr. Konrad Sandhoff
2. Referent: Prof. Dr. Stefan Bräse
3. Referent: Priv. Doz. Dr. Gerhild van Echten-Deckert
4. Referent: Prof. Dr. Albert Haas

Datum der Promotion: 27. 03. 09

Table of Contents

1 Introduction

1.1 Biological membranes

Biological membranes consist of a continuous double layer of lipid molecules in which membrane proteins are embedded. The lipid compositions of the inner and outer monolayers also differ, reflecting the distinct functions of the two faces of a cell membrane. This lipid bilayer is fluid and amphipathic, with individual lipid molecules able to diffuse rapidly within their own monolayer. The lipid molecules with the most extreme asymmetry in their membrane distribution are the sugar-containing lipid molecules. With exception of glucosylceramide these molecules are found exclusively in the noncytosolic monolayer of the lipid bilayer, where they are thought to partition preferentially into lipid rafts. (Small region of the plasma membrane enriched in sphingolipids and cholesterol) (Ko et al. 1998).

There are three major classes of membrane lipid molecules—phospholipids, cholesterol, and glycolipids. In the plasma membrane, the oligosaccharide headgroups are exposed towards the extracellular surrounding, where they have important roles in interactions of the cell with its surroundings such as in microbial pathogenesis or signal transduction.

1.2 Glycosphingolipids

Glycosphingolipides (GSLs) which are anchored on the extracytosolic leaflet of the plasma membrane of eukaryotic cells. GSLs are composed of a ceramide moiety and a hydrophilic, extracellularly oriented oligosaccharide headgroup at the 1-hydroxyl moiety. On the cell surface GSLs serve not only for the cell-cell recognition but also as binding sites for toxin, virus and bacteria, which bind to the oligosaccharide headgroup of GSLs (Karlsson 1989). A subfamiliy of the GSLs are the gangliosides, which are composed of a glycosphingolipide with one or more sialic acids linked to the sugar chain. They have been found to be

highly important in immunology. Natural and semisynthetic gangliosides are considered potential therapeutics for neurodegenerative disorders (Mocchetti 2005).

De novo biosynthesis requires the coordinate action of several enzymes (Stoffel 1973; Stoffel and Bister 1974; Stoffel and Melzner 1980; Stoffel and Sticht 1967) including serin palmitoyl transferase and ceramide synthase to generate ceramide. This process begins with the condensation of serine and palmitoyl-CoA to form 3-ketosphinganine and is localized on the cytosolic face of the endoplasmic reticulum. 2-Ketosphinganine is reduced to the sphingoid base to D-erythro-sphinganine (Mandon et al. 1992) and acylated to dihydroceramide by ceramide synthase. Dihydroceramide is oxidized then by the dihydroceramide-desaturase to ceramide (Michel et al. 1997; Rother et al. 1992).

To date, six ceramide synthase isoenzymes have been described in vertebrates and many other homologues in other organisms such as yeast, drosophila. The vertebrate ceramide synthases are encoded by the longevity assurance (*lass*) genes 1–6 (Lahiri and Futerman 2005; Mizutani et al. 2005; Pewzner-Jung et al. 2006; Riebeling et al. 2003). Each isoenzyme shows group specificity for particular fatty acids, leading to the *lass* gene-controlled biosynthesis of ceramide and ceramide derivatives with a specific fatty acid composition. C16 ceramide is one of the main ceramide species which synthesis is catalyzed by the gene products of *lass 5* and *6*, while ceramides with longer chains such as C20 and C24 ceramides are mainly synthesized by *lass 2* and *4*, which are found in the hippocampus (Wang et al. 2008).

Ceramide synthesis occurs in the endoplasmic reticulum (ER) and that of sphingomyelin and complex GSLs in the Golgi apparatus. As the hydrophobic nature of ceramide prevents its spontaneous transfer through the cytosol (Venkataraman and Futerman 2001), it must travel from the ER to the Golgi

apparatus by facilitated mechanisms. This was demonstrated to occur by both vesicular and non-vesicular transport (Fukasawa et al. 1999).

Of great importance is the isolation and characterization of a protein, CERT, previously called the Goodpasture antigen-binding protein that transports ceramide between the ER and the Golgi apparatus (Hanada et al. 2003). The two important binding domains of CERT are the pleckstrin homology (PH) domain, which targets the proteine to the Golgi, and the steroidogenic acute regulatory protein (STAR)-related lipid transfer (START) domain, a conserved lipid-binding domain that associates with sterols and ceramide (Bieberich 2008; Kudo et al. 2008). It is assumed that ceramide transported by CERT is used for sphingomyelin biosynthesis while that converted to glycosphingolipids follows the classical vesicular route (Hanada et al. 2003; Kumagai et al. 2005).

At this point, it should be noted that ceramide may also distribute throughout specialized ER compartments, such as the perinuclear membrane and the mitochondrial-associated ER membrane (MAM).(Bieberich 2008) This latter point is particularly important as evidence is now emerging that sphingolipid metabolism can occur in unexpected subcellular locations such as in the nucleus and in mitochondria (Bionda et al. 2004), and not just in the sub-fractions of the ER membrane that are tightly associated with these organelles, although it is not entirely clear whether ceramide is synthesized in these organelles or transported from the ER (Albi et al. 2006; Albi et al. 2008; Bionda et al. 2004; Ledeen and Wu 2006, 2008). A neutral ceramidase has also been found in mitochondria (El Bawab et al. 2000), and there is evidence for a sphingomyelin cycle in the nucleus (Watanabe et al. 2004). Recent studies suggest that ceramide is involved in the initiation of apoptosis by forming pores in the outer mitochondrial membrane (Siskind et al. 2006).

At present, nothing is known about whether CERT, or perhaps other putative ceramide-binding proteins, is involved in regulating ceramide levels in any of the intracellular signalling pathways in which it is involved.

After transport to the Golgi apparatus, ceramide is glycosylated on the cytosolic side of the Golgi apparatus to glucosylceramide. Although it may be regulated this transbilayer movement becomes a rate-limiting step (Hannun and Obeid 2008). In the Golgi lumen, sphingomyelin is synthesized by sphingomyelin synthase (SMS)1 and then transported to the cell membrane) (Ding et al. 2008; Guillen et al. 2007; Tafesse et al. 2006). SMS1 is distinct from SMS2, which regenerates sphingomyelin from ceramide in the cell membrane (Bieberich 2008; Huitema et al. 2004; Vos et al. 1995).

The biosynthesis of higher GSLs takes place in the lumen of the Golgi apparatus. They are synthesized by sequentially acting, membrane-bound glycosyltransferases and transported to the cell surface by a vesicular membrane flow (Schwarzmann and Sandhoff 1990).(Fig. 1-1)

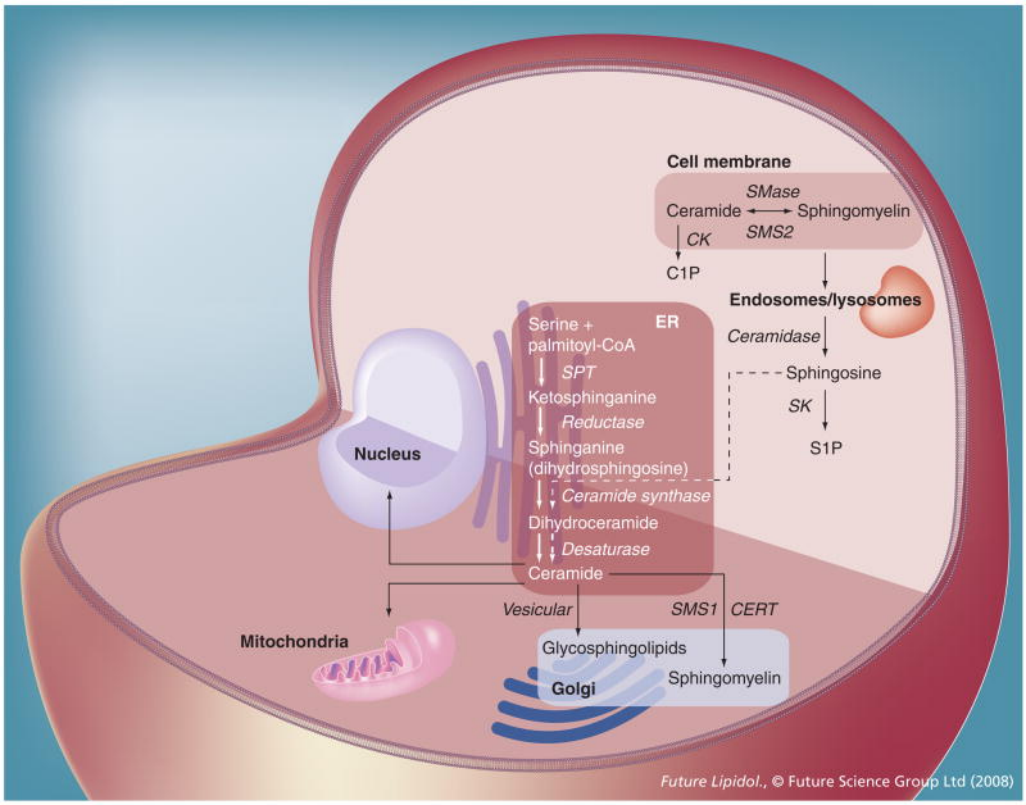

Fig. 1-1 In the Golgi, ceramide is used as precursor substrate for glycosphingolipid and sphingomyelin biosynthesis. Sphingomyelin is then transported to the cell membrane. Ceramide generated by the degradation of sphingomyelin in the endosomal/ lysosomal pathway can be hydrolyzed to sphingosine and recycled back

to the ER mediated by the ‘salvage pathway’ (dashed arrows). Ceramide generated in the ER can be transported to the nucleus (via perinuclear ER cisternae) and the mitochondria (via mitochondrial-associated ER membrane). Ceramide can also be converted to ceramide 1-phosphate (C1P) or to sphingosine and subsequently to sphingosine 1-phosphate (S1P) CERT: Ceramide transport protein; CK: Ceramide kinase; SK: Sphingosine kinase; SMase: Sphingomyelinase; SMS: Sphingomyelin synthase; SPT: Serine palmitoyltransferase. From (Bieberich 2008))

In terms of complexity, at least five different sphingoid bases are known in mammalian cells, more than 20 species of fatty acids, which are varying in chain length, degree of saturation, and degree of hydroxylation, can be attached to the sphingoid base, and around 500 different carbohydrate structures have been described in GSLs, although there is often some preference for association of specific components in specific sphingolipids.

The degradation of plasma membrane-derived GSLs takes place in the acidic compartments (late endosome and lysosome) of the cell (Zeller and Marchase 1992); (Sandhoff and Kolter 2003). According to a hypothesis for the topology of lysosomal digestion, GSLs are internalized from the plasma membrane and transported to lysosomes through the endocytotic pathway as membrane-bound components of intraendosomal and intralysosomal vesicles (Furst and Sandhoff 1992), which bud from the endosomal membrane into the endosomal lumen and are presumably engulfed in budding vesicles to be transported to the lysosomes. These vesicles might fuse with the lysosoms releasing the intralysosomal vesicles into the lysosol where the lipids are in the correct orientation to be degraded (Fig. 1-2). The lysosomal perimeter membrane, however, is protected from degradation by a glycocalix composed of the oligosaccharide headgroups of LIMPs (lysosomal integral membrane proteins) and LAMPs (lysosomal associated membrane proteins; (Carlsson and Fukuda 1990; Linke 2000)

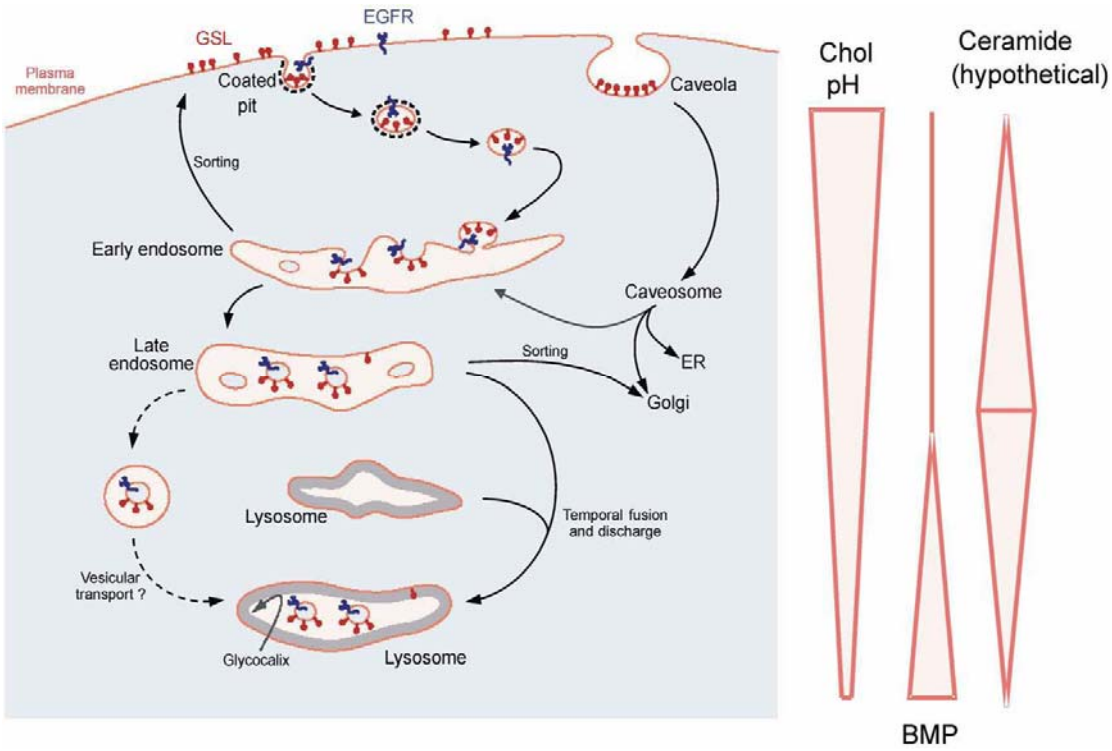

Fig. 1-2: Model for the topology of lysosomal GSL digestion. Parts of the plasma membrane, including GSLs, are incorporated into the membranes of intra-endosomal vesicles and membrane structures during endocytosis. The vesicles reach the lysosomal compartment when late endosomes are transiently fused with primary lysosomes and are degraded there, adapted from (Kolter and Sandhoff 2005). GSL: Glykosphingolipide, EGFR: epidermal growth factor receptor (Möbius et al. 2003; Schulze et al. 2008)

The lysosomal degradation of GSLs with oligosaccharide headgroups and of the sphingolipid ceramide is a sequential pathway. For the degradation of the GSL with short oligosaccharide headgroups several of these enzymes requires the coordinate action of acidic hydrolases and sphingolipid activator proteins (SAPs), (Linke et al. 2001). The SAPs are small glycoproteins, the saposins Sap-A, -B, -C,-D and the GM2-activator protein (Sandhoff et al. 2001).

1.3 Sphingolipid activator proteins (SAPs)

Sphingolipid activator proteins (Saposin) are highly homologous, small, nonenzymatic proteins. They belong to the large and divergent family of saposin-like proteins (SAPLIPs) and domains containing the ‘‘saposin fold’’

characterized by four or five adjacent amphipathic α helices forming bundles stabilized by conserved disulfide bridges or by cyclization (Gonzalez et al. 2000). The all-helical core structure of SAPLIPs is adapted to carry out a number of different functions at biological membranes.

Despite their similar structures, each saposin promotes the degradation of particular sphingolipids by a specific enzyme or partially overlapping sets of enzymes (Kolter et al. 2005). Current models for enzyme activation address the location of saposin-mediated lipid–hydrolase interactions and define the ‘‘solubilizer’’ and ‘‘liftase’’ modes of action (Wendeler et al. 2004; Wendeler et al. 2006). In the former model, target lipid molecules are extracted from bilayers by saposins and presented to cognate enzymes as soluble protein–lipid complexes. In contrast, the ‘‘liftase’’ model involves the binding of enzyme to the bilayer surface where saposin molecules facilitate the access to the glycosphingolipid substrates. For example, Sap-B is thought to be a detergent-like lipid solubilizer (Remmel et al. 2007; Yuan et al. 2007), whereas Sap C may act as a liftase at the bilayer surface (Wilkening et al. 1998).

Sap-D is involved *in vivo* in ceramide hydrolysis by acid ceramidase, it enhances the degradation of ceramide both in cell culture and in vitro (Klein et al. 1994; Linke et al. 2001). However, the exact mode of ceramidase activation by Sap-D has not yet been investigated in detail and will be subject of the following thesis.

1.4 The salvage pathway

In addition to sphinganine, ceramide synthase accepts sphingosine as a substrate for the acylation reaction, which is an essential step in so called salvage pathway of ceramide biosynthesis (Fig. 1-3). Sphingosine serves as the product of sphingolipid catabolism, and it is mostly salvaged through reacylation, resulting in the generation of ceramide or its derivatives (Gillard et al. 1998a; Gillard et al. 1998b; Gillard et al. 1996; Kitatani et al. 2008). This

recycling of sphingosine is termed the "salvage pathway", and recent evidence points to important roles for this pathway in ceramide metabolism and function since many processes involving ceramide as an apoptosis inducer appear to be related to ceramide in a perinuclear, possibly endosomal, compartment (Kitatani et al. 2008).The salvage pathway is also interesting with respect to the fatty acid specificity of ceramide synthase.

A number of enzymes are involved in the salvage pathway, and these include sphingomyelinases, cerebrosidases, ceramidases, and ceramide synthases. Recent studies suggest that the salvage pathway is not only subject to regulation, but it also modulates the formation of ceramide and subsequent ceramide- derivatives to proapoptotic ceramide and ceramide dependent cellular signals.

Before the salvage pathway can utilize ceramide, it has to be converted into its derivatives. To achieve this, ceramide is transported from the ER to the Golgi apparatus following two distinct transport routes.

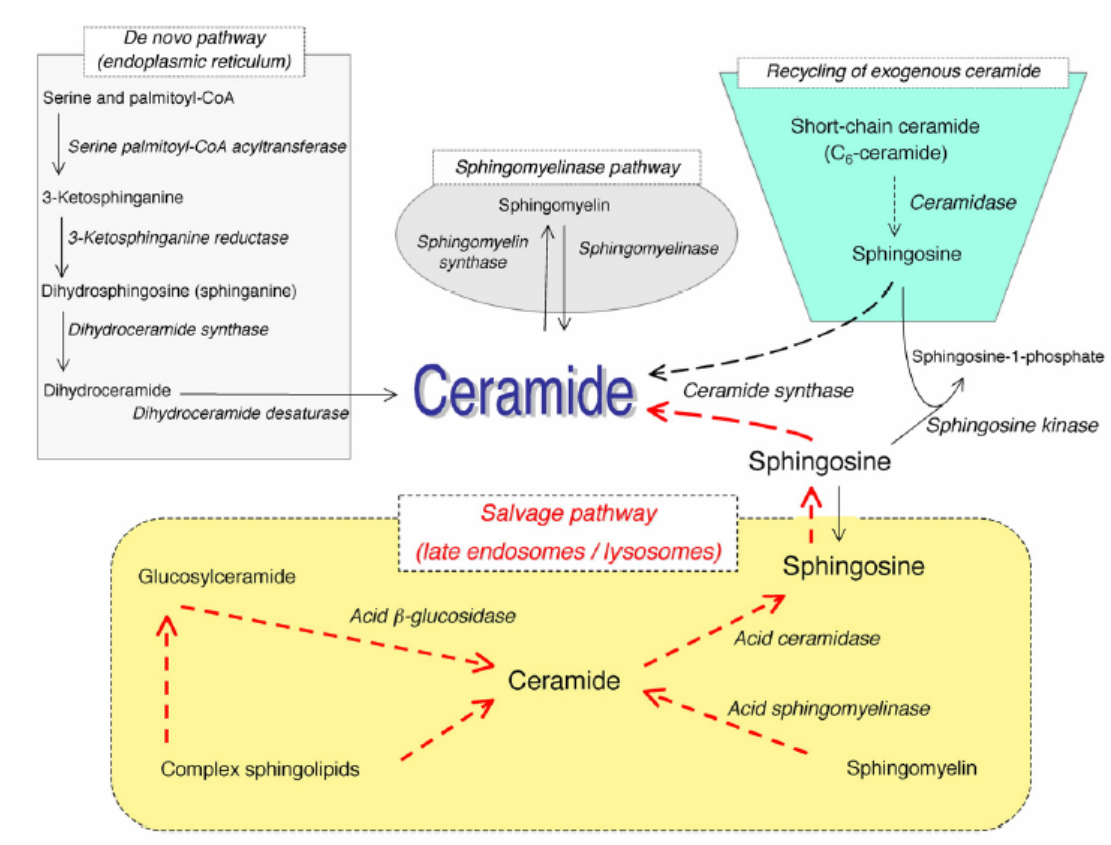

Fig. 1-3: The salvage pathway. Depicted are the metabolic pathways for ceramide synthesis as well as the de novo pathway and the exogenous ceramide-recycling pathway, and the salvage pathway. Dotted lines indicate the recycling/salvaging pathway of ceramide synthesis. From (Kitatani et al. 2008)

1.5 Ceramides and ceramidases

Ceramides are important building blocks of eukaryotic membranes. It is assumed that they are segregated in microdomains in the lateral plane of the lipid bilayer that are enriched in other sphingolipids and cholesterol (Munro 2003). Some of the microdomains were believed to be tightly packed, ordered membrane domains that are generally enriched in both lipids with saturated acyl chains (e.g., sphingolipids) and sterol (London 2002; Schroeder et al. 1994). They are believed to segregate from disordered membrane domains that are rich in lipids with unsaturated acyl chains (London 2002; Megha et al. 2007). Their formation might be driven, at least in part, by the affinity of

cholesterol for specific sphingolipids, although the precise biophysical rules that determine how cholesterol interacts with different sphingolipids have not yet been fully elucidated and may yield surprises. During the last few years it became clear, that lipid microdomains are complex dynamic structures in membranes, in which lipids and proteins are interacting in order to express their function. So far it is known that there are different forms of such microdomains. Lipid-lipid interactions play a major role in lipid phase separation. Among others liquid ordered and liquid disordered phases depend on the physical conditions such as temperature and lateral pressure, and the types of lipids. Other membrane domains are due to protein-protein interactions. A third type of microdomains results form lipid-protein interactions, which tend to form so called lipid shells to improve the protein activity

(AFM) and Fluorescence-Correlation Spectroscopy (FCS) as well as emission depletion (STED) far-field fluorescence nanoscopy studies showed that unlike phosphoglycerolipids, sphingolipids are transiently (10–20 ms) trapped in cholesterol-mediated molecular complexes within 20-nm diameter areas. Only long chain ceramides, with a backbone of 16 to 18 carbon atoms, can segregate from the other lipids of a membrane bilayer composed of SM, DOPC and cholesterol and form ceramide-enriched domains (Chiantia et al. 2007; Chiantia et al. 2008; Eggeling et al. 2008). However, it is also now becoming evident that the detergent resistant membranes (DRMs) often called as “Lipid rafts” and lipid microdomains are two different concepts, albeit possibly having certain properties or components in common. Up to now, there is no proof that lipid rafts exist in the plasma membrane of living cells (for review see (Gallala and Sandhoff 2008))

Under some conditions it has been reported that activation of SMase leads to the generation of ceramide-rich membrane domains on the plasma membrane, which can exist in the form of large ceramide-rich platforms (Grassme et al. 2001; Grassme et al. 2003). The formation and functional role of ceramide-rich

domains have been reviewed recently (Bollinger et al. 2005; Gallala and Sandhoff 2008).

Natural ceramide has a long saturated *N*-acyl chain and small polar headgroup, making it a lipid with very tight packing properties. Model membranes composed of ceramide have a high order-to-disorder transition temperature (Megha et al. 2007; Shah et al. 1995). Surprisingly, long chain ceramide has the ability to stabilize and promote microdomain formation in model membranes (Megha and London 2004; Xu et al. 2001) and have the ability to displace sterols from lipid microdomains, a fact that seems to be relevant for the degradation of intralysosomal membranes (Alanko et al. 2005; Megha and London 2004; Yu et al. 2005). Some years ago, a gradual displacement of sterol has also been observed in endocytic membranes on their way to the lysosomes by Möbius et al. in electron microscopy studies (Möbius et al. 2003). While early endosomes still contain sterols in high amounts, they will be displaced by ceramide, when the intralysosomal membranes are formed. The sterols must be recycled from the endosomal compartment. (Megha et al. 2007)

Ceramides are not only components of the membrane structure, they also are involved in several signaling pathways and microbial pathology (Heung et al. 2005) The levels of ceramide *in vivo* are carefully regulated. Hannun and coworkers provided evidence that ceramide is a second messenger (Okazaki et al. 1990). So far, not only ceramide but also its metabolites such as ceramide 1-phosphate, sphingosine, and sphingosine 1-phosphate (S1P) are now recognized as messengers playing essential roles in events as diverse as differentiation, senescence, proliferation, and cell cycle arrest cell growth, survival, and death (Hannun et al. 2001; Mathias et al. 1998). In contrast to ceramides those ceramide metabolites contain a hydrophilic region such as phosphate in the case of sphingosine-1-phosphate (S1P) and ceramide-1-phosphate as well as the phosphorylcholin in sphingomyelin.

Phosphorylation of the ceramide is catalyzed by ceramide kinase (Hannun et al. 2001; Mathias et al. 1998), while deacylation occurs by either neutral or acid ceramidase yielding sphingosine, which may be phosphorylated by sphingosine kinase to S1P by the so far two known sphingosine kinases, which differ in temporal patterns of appearance during development, are expressed in different tissues, and possess distinct kinetic properties (Liu et al. 2000).

While ceramide is often antiproliferative and proapoptotic, S1P plays a role in cellular proliferation and survival (Olivera and Spiegel 1993), and in protection against ceramide-mediated apoptosis (Cuvillier et al. 1996). A growing body of evidence is starting to point toward roles for ceramide generated through the salvage pathway in many biological responses, such as growth arrest (Ogretmen et al. 2002), apoptosis (Takeda et al. 2006), cellular signaling (Kitatani et al. 2006), and trafficking (Becker et al. 2005; Kitatani et al. 2006)

Sphingosine itself has been proposed to induce apoptosis (Cuvillier 2002; Cuvillier et al. 2000; Cuvillier et al. 2001) independent of ceramide.

However, it has been recently shown that ceramide induces autophagy in mammalian cells and that ceramide might kill mammalian cells by limiting cellular access to extracellular nutrients. Edinger et al. have found that ceramide starves cells to death subsequent to profound nutrient transporter down-regulation. In mammalian cells, a lethal dose of ceramide triggers a bioenergetic crisis by so severely limiting cellular access to extracellular nutrients that autophagy is insufficient to meet the metabolic demands of the cell (Edinger 2009; Guenther et al. 2008).

As described above ceramide may be formed by several pathways, but the only way to degrade ceramide into sphingosine is through the activity of different ceramidases. These enzymes display a non peptide-specific amidase activity and are divided into three different species, an alkaline, a neutral, and an acid ceramidase. The best-characterized form is the human acid

ceramidase. Human acid Ceramidase (N-Acetylsphingosine amidohydrolase, EC 3.5.1.23) catalyzes the hydrolysis of ceramide to sphingosine and free fatty acid (Fig. 1-4).

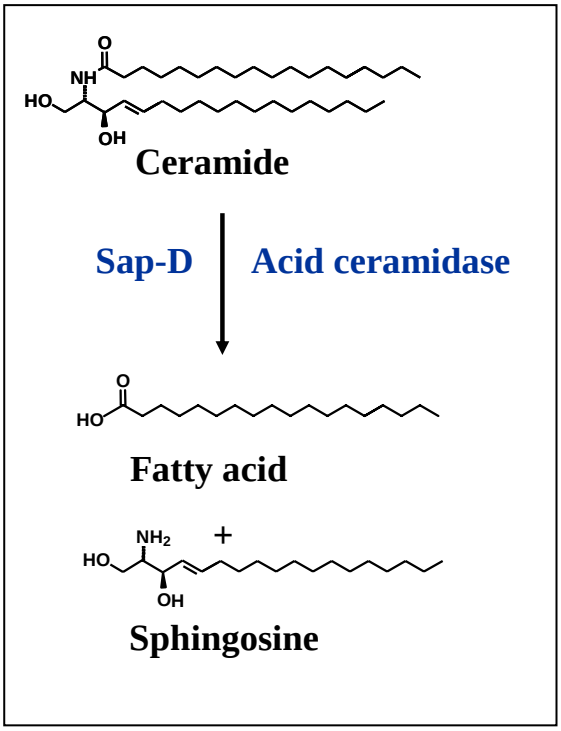

Fig. 1-4: The acid ceramidase catalyzes the hydrolysis of the amide-bond in ceramide with the presence of the sphingolipid activator proteins, Sap-D.

Its deficiency or defect in humans results in Farber's disease (Bär et al. 2001; Farber 1952; Zhang et al. 2000), a sphingolipidosis with accumulation of ceramide in various tissues, including liver, lung, and spleen. The phenotype of this rare sphingolipid storage disease is mainly attributed to deformed joints and skin lipogranulomatosis with subcutaneous nodules.

Besides the sequencing and mapping of the gene (Li et al. 1999), the full-length cDNA encoding 395 amino acids was isolated (Koch et al. 1996). In addition, extensive cloning approaches as well as many genome projects led to the discovery and isolation of mouse (Li et al. 1998), rat (Mitsutake et al. 2001), Drosophila (Yoshimura et al. 2002), and bacterial ceramidases

displaying an acidic pH optimum. Likewise, ceramidases with neutral and alkaline pH optima have been discovered (Mao et al. 2001), which do not relate with the acidic forms in their primary amino acid structure indicating their distinct roles and subcellular locations. While one alkaline ceramidase have been shown to be highly expressed in the skin (Mao et al. 2003), another distinct alkaline ceramidase possesses a substrate specificity to phytoceramide (Mao et al. 2001). There are also distinct forms of the neutral ceramidases. Thus, one form is a type II integral membrane protein that can be cleaved to reveal a secreted isoform (Tani et al. 2003) and expresses its main function in the digestion of the dietary sphingolipids in the gut (Kono 2006), while another is located to mitochondria (Kono et al 2006, el Bawab 2000). One form of the neutral ceramidases is located to the mitochondria , where it is breaks down ceramide to sphingosine (Bionda et al. 2004; El Bawab et al. 2000). In addition, mitochondria contain enzymes capable of generating ceramide (ceramide synthase and reverse ceramidase) and several apoptotic stimuli have been shown to cause an elevation of mitochondrial ceramide that precedes the mitochondrial phase of apoptosis (Raisova et al. 2000). It is assumed that ceramides form oligomeric barrel-stave channels in planar phospholipid membranes (Siskind et al. 2003). In mitochondrial outer membranes, ceramide channels allow the release of proteins up to 60 kDa in size (Siskind et al. 2002).

Acid ceramidase was first enriched in 1963 by Gatt and colleagues, but first purified to homogeneity from human urine in 1995 (Bernardo et al. 1995) and from placenta in 2000 (Linke et al. 2000).

Human acid ceramidase is expressed as a 55 kDa protein, which is maturated in the secretory pathway. (Fig. 1-5) After internalization into the ER the N-terminal signal peptide is removed yielding the 53 kDa enzymatically inactive precursor form, which is glycosylated and transported via the mannose-6-phosphate receptor pathway to the endosomal/ lysosomal

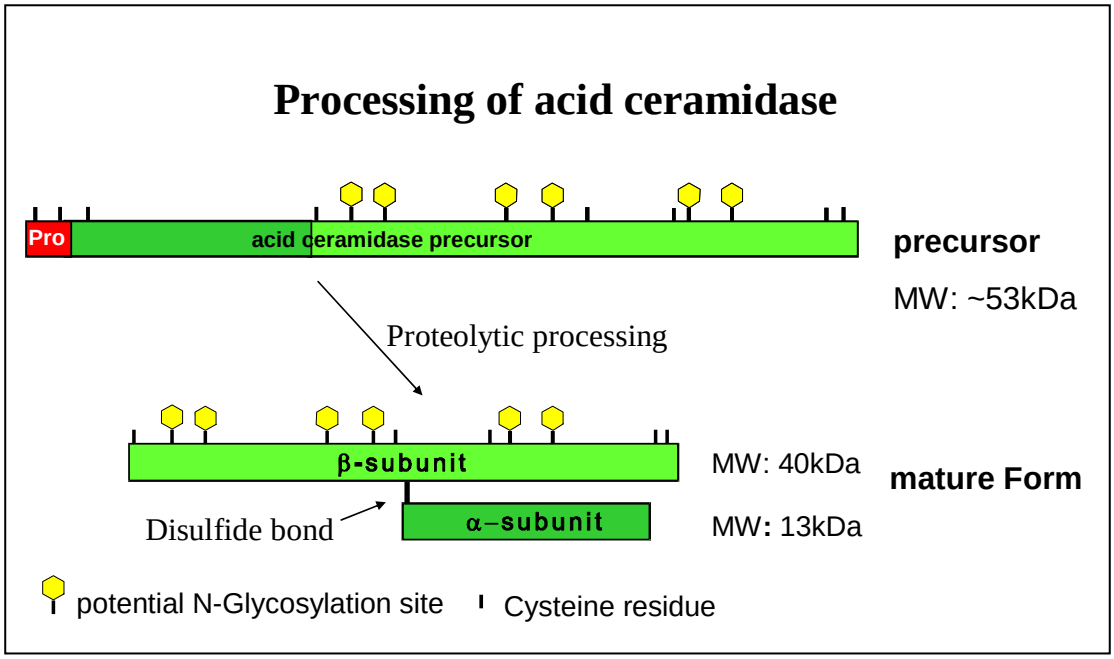

Fig. 1-5: Schematic illustration of the acid ceramidase processing, adapted from (Bär et al. 2001).

compartments, where it is processed into its active form (Ferlinz et al. 2001). The mature active form of human acid ceramidase is generated by the cleavage of the precursor protein to yield a heterodimer consisting of two different subunits α (MW: ~13kDa) and β (MW: ~40kDa) within the endosomal/ lysosomal pathway and deglycosylation of purified human acid ceramidase with endoglycosidase H or peptide-N-glycanase F reduces the molecular weight of the β-subunit to approximately ~30-35 kDa and to ~27 kDa, respectively (Linke 2000). The cleavage site was reported to be Ile-142 – Cys-143 (Ferlinz et al. 2001; Schulze et al. 2007) revealing the unglycosylated α-subunit (molecular mass, 13 kDa) and glycosylated β-subunit (40 kDa; peptide backbone, 28 kDa). Both subunits are linked by a single disulfide bridge (Schulze et al. 2007).(Fig. 1-6)

.

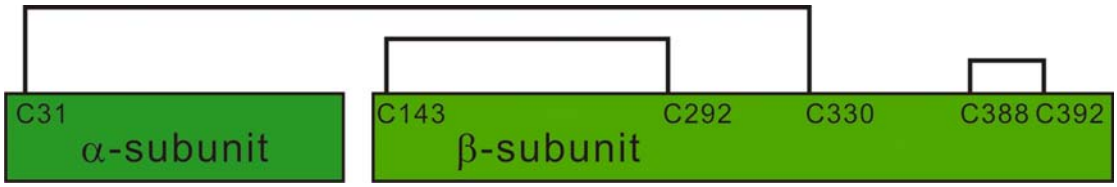

Fig. 1-6: Disulfide pattern derived from mass spectrometry according to Schulze et al., 2007.

Mass spectrometry on tryptic and chymotryptic digest of recombinant acid ceramidase located this disulfide bridge. Studies, with recombinant human acid ceramidase overexpressed in Sf9 insect cells have shown that this cleavage and the conversion into the heterodimer also occur in vitro after acidification of the Sf9 culture medium to pH 4-5. Some lysosomal enzymes such as lysosomal N-acylethanolamine hydrolyzing acid amidase (NAAA), cathepsin L, and tripeptidyl-peptidase I were also reported to be subjected to *in vitro* processing under acidic conditions and activated by the cleavage. Further, the mass spectrometry apprpoach revealed a detailed mapping of the other disulfide bridges and the glycosylation patterns. Human acid ceramidase has six potential N-glycosylation sites, five of which were reported to be actually glycosylated by complex glycostructures (Ferlinz et al. 2001; Schulze et al. 2007).

1.6 Ntn (N-terminal nucleophile)-Hydrolase

Recently, it was shown that acid ceramidase exhibits 33–35% amino acid identity to the lysosomal N-acylethanolamine hydrolyzing acid amidase (NAAA), an amidase specific for N-palmitoyllethanolamine and other linear N-acylethanolamines and anandamides.

The conspicuous sequence similarity of between human acid ceramidase and human NAAA as well as the homology of the N-terminal sequence to NAAA (Tsuboi et al. 2007), the bile salt hydrolase (BSH) (Rossocha et al. 2005) and penicillin V acylase (PVA) suggested that the ceramidase would belong to the

choloylglycine hydrolase family (Pfam PF02275), a subfamily of the N-terminal nucleophile (Ntn) hydrolase superfamily. The Ntn-hydrolases display a wide range of substrate specificity and resemble enzymes besides the ones mentioned above as diverse as the proteasome subunits (Bochtler et al. 1999; Seemuller et al. 1996), the lysosomal aspartyl glucosaminidase, the glutamine PRPP amidotransferase, and the fatty acid amide hydrolase (FAAH).

Despite their insignificant homology in the primary structure, they share highly conserved motifs such as the N-terminus and other residues involve in the catalytic center and show an overall high similarity in the tertiary four-layered $\alpha\beta\beta\alpha$ sandwich structure and quarternary tetrameric structure (Rossocha et al. 2005). They all catalyze the hydrolysis of amide bonds present in proteins and other amides such as lipids, bile salts, and other small molecules. They also share similar self-activation and catalytic mechanisms (Brannigan et al. 1995; Oinonen and Rouvinen 2000). Usually, Ntn-hydrolases are synthesized as pre-proteins, which are endoproteolytically processed to their active form. This process is autocatalytic generating an N-terminal residue, which is acting as a nucleophile. For NAAA, BSH, and PVA, a cysteine has been shown to be the first residue of the mature protein. Crystal structures of BSH, PVA, and others members of this family have proven that this residue is central to the mechanism of catalysis and serves both as a nucleophile and as a proton donor (Kumar et al. 2006; Rossocha et al. 2005). The N-terminal amino group acts as the proton acceptor and activates the nucleophilic thiol group of the Cys side chain. The N-terminal cysteine becomes a catalytic center only upon removal of the initiation formylmethionine. Such unmasking post-translational modifications are common to all members of the Ntn hydrolase superfamily. Furthermore, Ntn-hydrolases, they all catalyze the amide bond hydrolysis, but they differ in their substrate specificities. The catalytic machinery is located in the structures in a similar manner: the N-terminal residue of Ntn-hydrolase

functions as a nucleophile and as a catalytic base (Fig. 1-7). The reactivity of this nucleophile is affected by the amino acid residues interacting in the vicinity. During the reaction, a covalent intermediate is formed via a transition state, which is stabilized by residues from the oxyanion hole (Peräkylä et al 1997). The importance of the Cys -SH group was confirmed by mutagenesis that replacement of Cys with other potential nucleophilic residues such as Ser or Thr resulted in the loss of BSH activity. The removal or exchange of the nucleophilic residues by Ala, Ser, or Thr resulted in the loss of activity as it has been shown for BSH and NAAA.

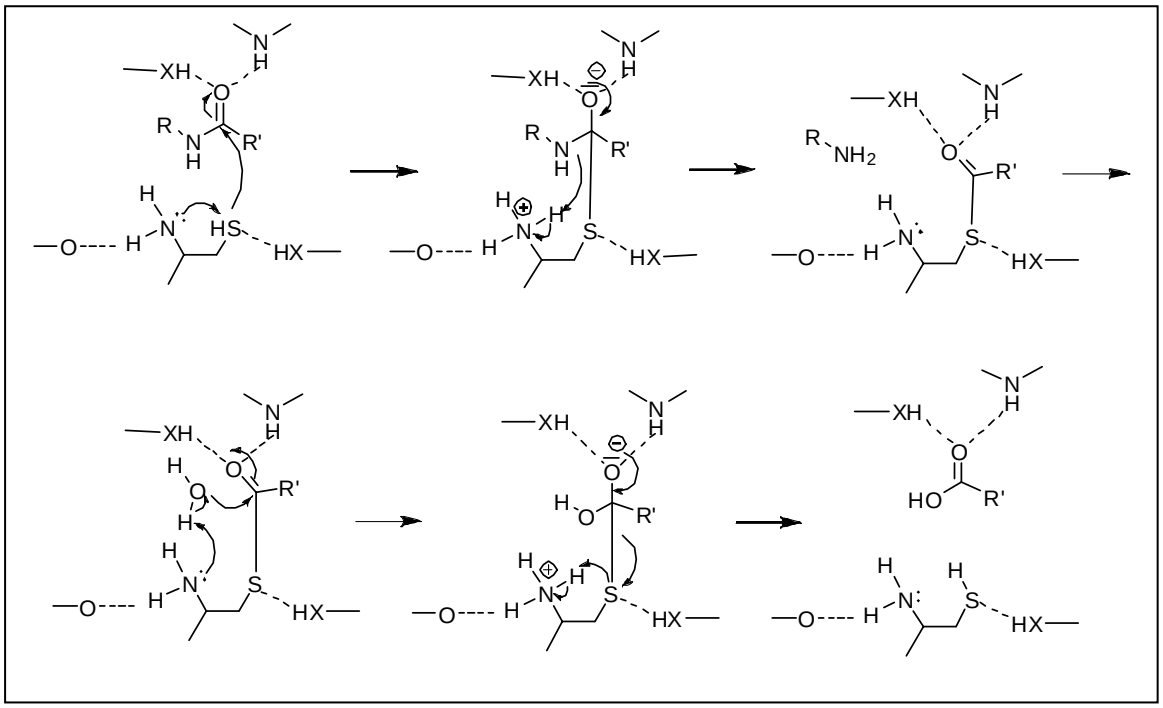

Fig. 1-7: Catalytic mechanism of Ntn-hydrolases: Y represents oxygen or sulfur, and X represents nitrogen or oxygen. The reaction begins when the nucleophilic oxygen/sulfur of Thr/Ser/Cys donates its proton to its own α-amino group and attacks the carbonyl carbon of the substrate. The negatively charged tetrahedral intermediate is stabilized by hydrogen bonding (oxyanion hole formers). The acylation step is complete when the α-amino group of the Thr/Ser/Cys donates the proton to the nitrogen of the scissile peptide bond. The covalent bond between the part of the substrate and the enzyme is formed and the part of the substrate is released. The deacylation step begins when the hydroxyl group of water attacks the carbonyl carbon of the acyl-enzyme product, and the basic α-amino group of the nucleophile accepts the proton from the water molecule. The negatively charged intermediate is stabilized,

as in the acylation step. The reaction is complete when the α-amino group donates the proton to the nucleophile. Adapted from (Oinonen and Rouvinen 2000)

1.7 Objective

Human acid ceramidase hydrolyzes the sphingolipid, ceramide, into sphingosine and free fatty acid. The mature acid ceramidase consists of two subunits, which were derived from a single precursor by proteolytic processing. However, the mechanism of acid ceramidase precursor cleavage remains unclear. In addition, PSI-BLAST search (Altschul et al. 1997) for the acid ceramidase sequence revealed high homology with the N-terminal nucleophile (Ntn) hydrolase. For example, acid ceramidase exhibits 33–35% amino acid identity to the lysosomal N-acylethanolamine hydrolyzing acid amidase (NAAA), the conspicuous sequence similarity between human acid ceramidase and human NAAA as well as the homology of the N-terminal sequence to NAAA (Tsuboi et al. 2007), the bile salt hydrolase (BSH) (Jones et al. 2008), and penicillin V acylase (PVA) suggested that the ceramidase would belong to the choloylglycine hydrolase family. For NAAA, BSH, and PVA, a cysteine has been shown to be the first residue of the mature protein, which is acting as a nucleophile. Crystal structures of BSH, PVA, and others members of this family have proven that this Cys residue is central to the mechanism of catalysis and serves both as a nucleophile and as a proton donor (Kumar et al. 2006); (Chandra et al. 2005).

Therefore, to prove whether the ceramidase belongs to the same family further analyses will be necessary to clarify the physiological significance of the cleavage of ceramidase. For this purpose, we established the recombinant expression and purification of the human acid ceramidase precursor to further study the structure by crystallization and the function of its variants comprising mutations of the Cys 143 residue, known as the N-terminal residue of the β-subunit, and mutation of the amino acids next to the cleavage site.

It has been shown that saposin D is involved *in vivo* in ceramide hydrolysis by acid ceramidase (Linke et al. 2001), but it is still unclear whether Sap D and acid ceramidase have *in vivo* protein-protein interaction or affinity domains. The goal is to prove for this interaction using in vivo and in vitro cross-linking experimentsl between Sap D and acid ceramidase.

2 Results

2.1 Functional expression of recombinant fusion protein “SEAP-haCerase”

2.1.1 Generating the Recombinant Vector containing “SEAP-haCerase”

One of the main goal of this thesis was the expression of recombinant human acid ceramidase precursor in insect cells (Sf9) to yield sufficient amounts of homogeneous and monospecific enzyme for biophysical and for structural investigations. For these experiments the Bac-to-Bac® Baculovirus Expression System is designed to create a recombinant baculovirus for high-level expression of the gene of interest in insect cells (Invitrogen). We have already expressed human acid ceramidase in insect cells (Schulze et al. 2007), but following this procedure, we could not isolate pure precursor, due to the premature maturation of the ceramidase precursor already in the media, which may be triggered by mature ceramidase released from virus lyzed cells. Therefore, a new strategy must have been designed. We constructed the recombinant pFastBac Vector containing fusion DNA fragment of “SEAP-haCeramidase” (Fig. 2-1).

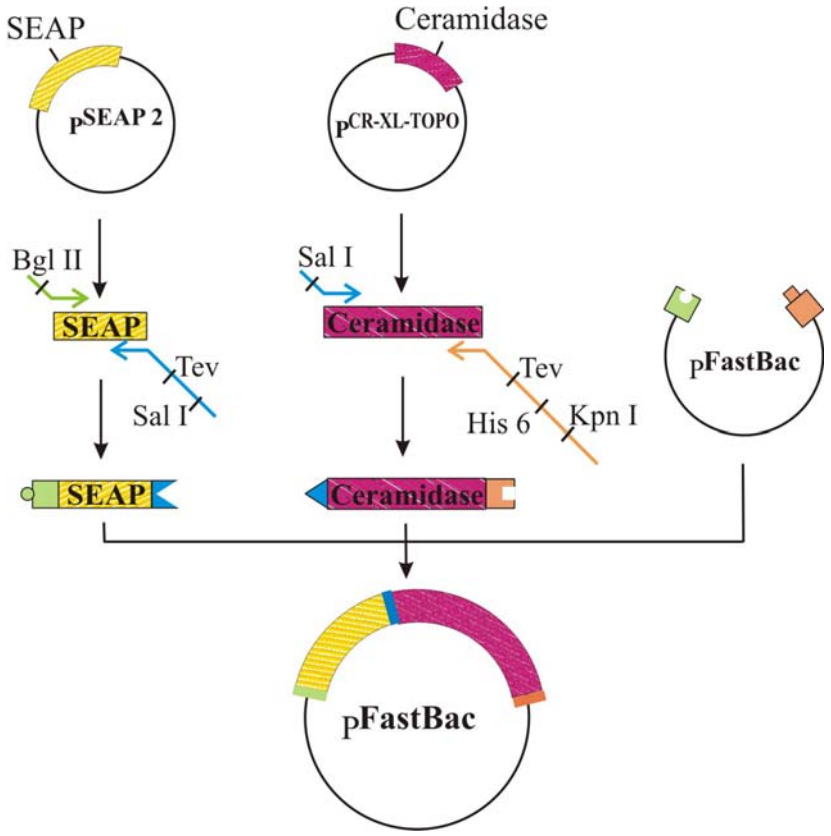

Fig. 2-1: PCR amplify our fragments of choice using designed primer and construct the pFastBac plasmid including the gene “SEAP-haCeramidase”

Due to the help of the secretory alkaline phosphatase (SEAP), which is only secreted into the medium, ceramidase will not occur in the lysosomes and maturation should be prevented. Sf9 cells infected with the recombinant baculovirus quickly secret a fusion protein “SEAP-haCerase” into the medium. Besides the SEAP secretion sequence the ceramidase DNA lacking its own ER-signal sequence also will contain a C-terminal His_6-tag for affinity purification and two Tev –sites for the recognition of a Tev-protease, a protease from the Tobacco etch virus, which will later be used for the removal of SEAP and the His-tag. Once the recombinant fusion protein is digested with Tev protease, the pure haCeramidase precursor will be isolated (Fig. 2-2).

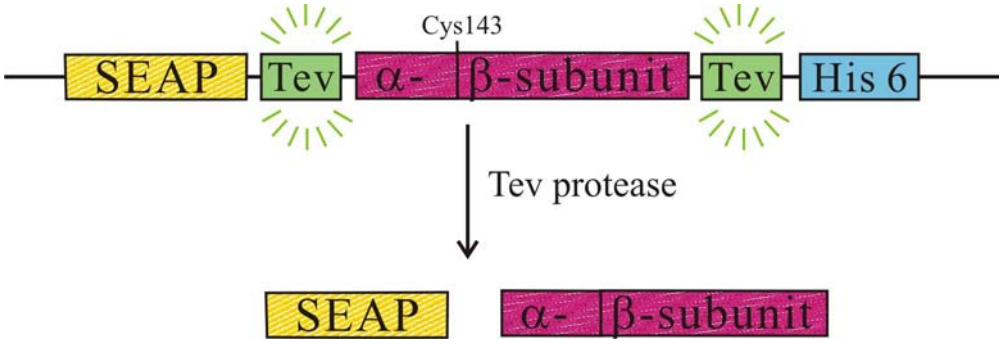

Fig. 2-2: After Tev protease digestion should haCeramidase precursor be obtained. **Tev:** a recognition sequence for tabacco etch virus (TEV) protease. **His 6:** allows purification of recombinant protein using Ni-NTA resin.

After PCR amplification of the ceramidase cDNA and the SEAP cDNA (see for primers and protocols in the Materials and Method section), restriction enzyme digestion and ligation of the insert DNA fragments, the recombinant fusion DNA fragment was inserted into the pFastBac™ vector, which is a baculavirus transfer vector. The successful cloning was confirmed by restriction-enzyme analysis to verify the presence of DNA fragment “SEAP-haCeramidase” already in the pFastBac™ vectors (Fig.2-3) and sequencing (Seqlab GmbH).

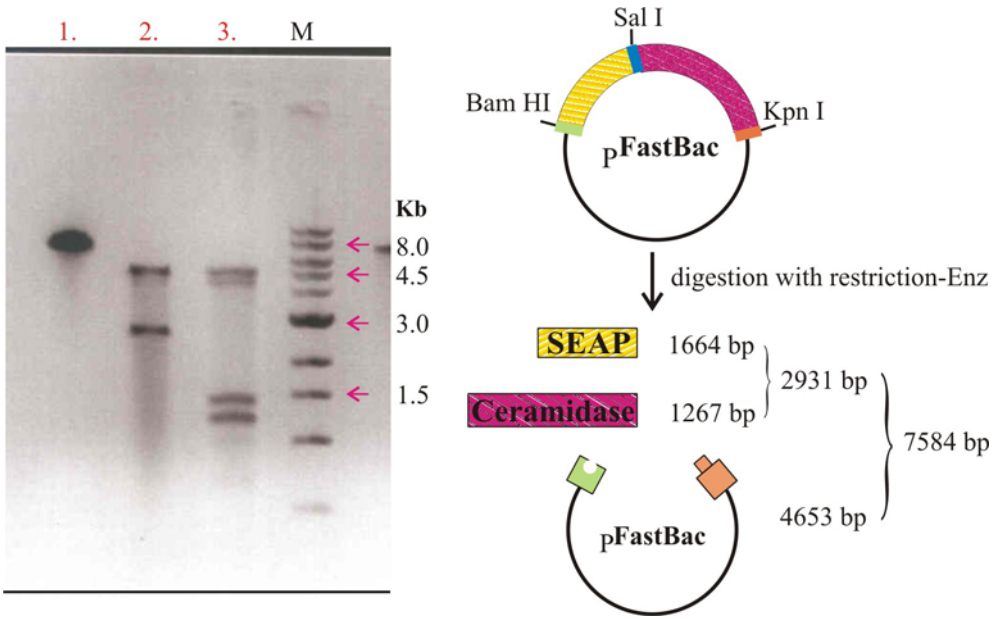

Fig. 2.3: After restriction enzyme digestion digested SEAP-ceramidase pFastBac clones were analyzed by agarose gel electrophoresis. Lane 1.: the recombinant pFastBac™ plasmid digested with Kpn I. Lane 2.: the same plasmid digested with Kpn I and Bam HI. Lane 3.: the same plasmid digested with Kpn I, Bam HI, and Sal I.

According to the result of restriction-enzyme analysis, the recombinant pFastBac™ vector with the fusion DNA fragment “SEAP-haCerase”was successfully constructed.

2.1.2 Expressing the recombinant fusion protein ”SEAP-haCerase”

Based on a method developed by Luckow 1993, the Bac-to-Bac baculovirus expression system takes advantage of the site-specific transposition properties of the Tn7 transposon (Luckow et al. 1993), which recognition site is present on the pFastBac transfer vector and on the baculogenome and allows the insertion of the pFastBac insert, here the SEAP-ceramidase into the baculo genome. In the Bac-to-Bac system the transposition can be performed in recombinant E.coli containing the modified baculo genome. Once transposition reaction was performed, the high molecular weight recombinant baculogenome DNA (bacmid) will be isolated and then transfected the bacmid

DNA into insect cells to generate a recombinant baculovirus. After the baculoviral stock is amplified and titered, this high-titer stock can be used to infect insect cells for high-level expression of the recombinant fusion protein.

This recombinant SEAP-ceramidase pFastBac™ vector was transformed into DH10Bac™ *E. coli* strain, which contained a baculovirus genome (bacmid) with a mini-*att*Tn7 target site and a helper plasmid. Transposition occurs between the mini-Tn7 element on the pFastBac™ vector and the mini-*att*Tn7 target site on the bacmid to generate a recombinant bacmid containing the fusion DNA fragment “SEAP-haCerase”. This transposition reaction occurs in the presence of transposition proteins supplied by the helper plasmid. Subsequently, as described above, the isolated recombinant bacmid DNA was transfected into Sf9 cells to generate a baculovirus containing DNA fragment “SEAP-haCerase”. The high-titer virus-stock infected Sf9 cells again to express the recombinant fusion protein “SEAP-haCerase” (Fig.2-4).

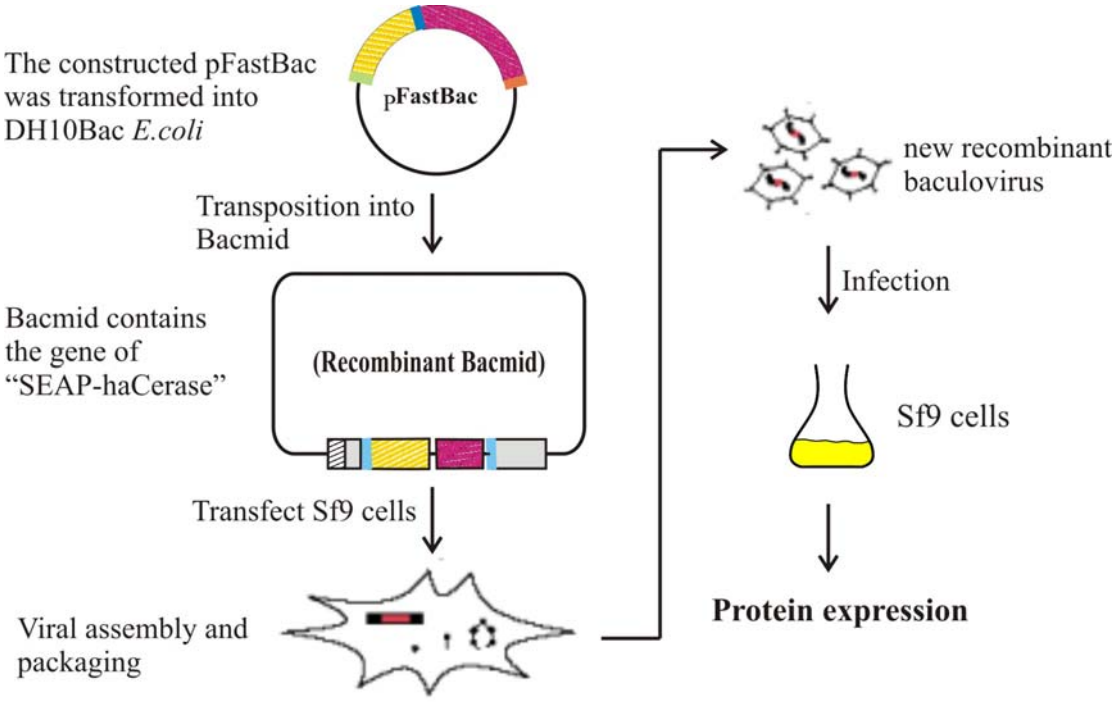

Fig. 2-4: Recombinant Bacmid DNA was transfected into insect cells to produce new recombinant baculovirus and then expression of recombinant fusioin protein “SEAP-haCerase”.

Once the baculoviral stock was generated, we used this new recombinant baculovirus to infect insect cells (Sf9) and analyzed the medium for the fusion protein “SEAP-haCerase”. Due to SEAP, the fusion protein was secreted into media, which was harvested 4 days post-infection (4-dpi). The identity of the fusion protein was ascertained by Western blot analysis with an anti-acid ceramidase rabbit antibody. SEAP-haCerase” was successfully synthesized as a 110 kDa fusion protein and Tev-protease digestion from the crude media revealed the cleavage from the fusion partners. However after 4-dpi there is still proteolytic cleavage of this protein into its heterodimeric mature form (40 kDa β-subunit and 70 kDa SEAP-α-subunit).

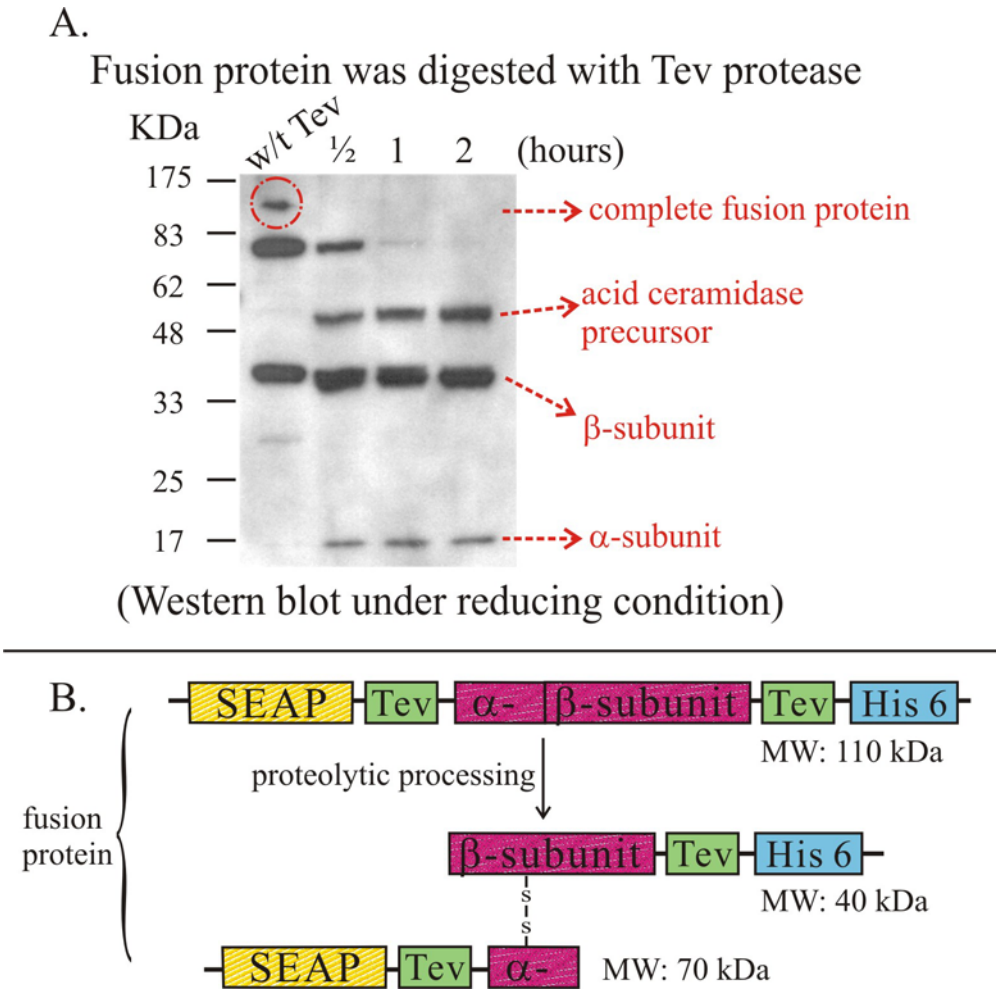

Fig. 2-5: (A.)Tev protease and Western blot analysis. Expression of the recombinant fusion protein in baculovirus-infected insect cells and then media was collected at 4

days. 30 µl samples were loaded onto 8% Tris/Tricine SDS-PAGE gel. Lane 1. the harvested media (4dpi) without Tev protease digestion, lane 2-4. time-course test with Tev protease. (B.) Illustration for proteolysis of fusion protein “SEAP-haCerase”.

2.2 Functional expression of a series of site-directed mutant fusion protein ”SEAP-haCerase”

2.2.1 Introducing point mutation into the acid ceramidase cDNA.

So far, the recombinant fusion protein was synthesized as a monomeric 110 kDa, but still a fast proteolytic process of this protein into heterodimeric units (40 kDa β-subunit and 70 kDa SEAP-α-subunit) occured in medium despite the help of the secretory alkaline phosphatase (SEAP). This was probably due to the fact that the proteolytic processing of acid ceramidase is occurring autocatalytically generating the N-terminal nucleophilic Cys of the β-subunit. Therefore, another new strategy for the expression of the acid ceramidase precursor had to be developed. We propose that proteolytic process of acid ceramidase should occur only under specific interaction among amino acids near cleavage site. To investigate this point, we make point mutations by mutating amino acids near the cleavage site to avoid proteolytic process of acid ceramidase.

According to chapter 2.1.1 the recombinant SEAP-ceramidase pFastBac™ plasmid was used as a template for constructing mutant expression plasmids by polymerase chain reaction (PCR). The designed primers and their antisense primers (Materials and Methods) were synthesized to introduce point mutations into the acid ceramidase cDNA through the QuickChange site-directed mutagenesis kit from Stratagene. The final PCR products, newly synthesized mutant-acid ceramidase cDNA constructs, were confirmed by sequencing (Seqlab GmbH). (Fig. 2-6)

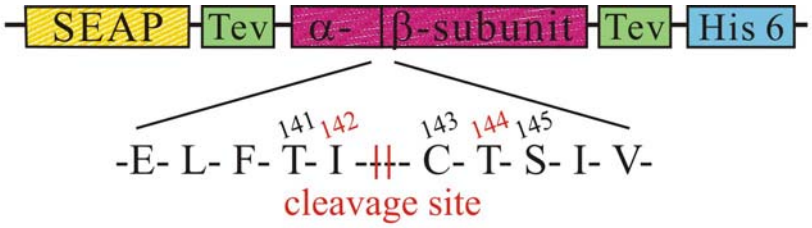

Mutation No.	Mutation in haCerase cDNA	Amino acid substitution
1	421 ACC → GTC	141 Thr → Val
2	424 ATT → GTT	142 Ile → Val
3	427 TGT → GCT	143 Cys → Ala
4	427 TGT → ATG	143 Cys → Met
5	430 ACT → GCT	144 Thr → Ala
6	433 TCA → GCT	145 Ser → Ala
7	433 TCA → ACT	145 Ser → Thr

Fig. 2-6: Site-directed mutagenesis of amino acids near the cleavage site between α- and β-subunit of acid ceramidase.

2.3 Expressing the mutant fusion protein ”SEAP-haCerase”

The confirmed mutant plasmids were then transformed into DH10Bac™ *E. coli* strain competent cells containing the baculovirus genome to generate a recombinant mutant SEAP-ceramidase bacmid. Subsequently, as previously described, the isolated recombinant mutant SEAP-ceramidase bacmid DNA was transfected into Sf9 cells to generate a baculovirus containing the mutant DNA region. The high-titer virus-stock infected Sf9 cells again to express the mutant fusion protein “SEAP-haCerase”. We produced a series of recombinant viruses expressing point-mutant variants of the SEAP-ceramidase protein. All variants were expressed in Sf9 insect cells. After 72 hours, the infected Sf9 cells were harvested by centrifugation (6000 rpm, 30 min). The supernatant including the mutant fusion proteins “SEAP-haCerase” was directly subjected to SDS-PAGE followed by Western Blot (Fig.2-7).

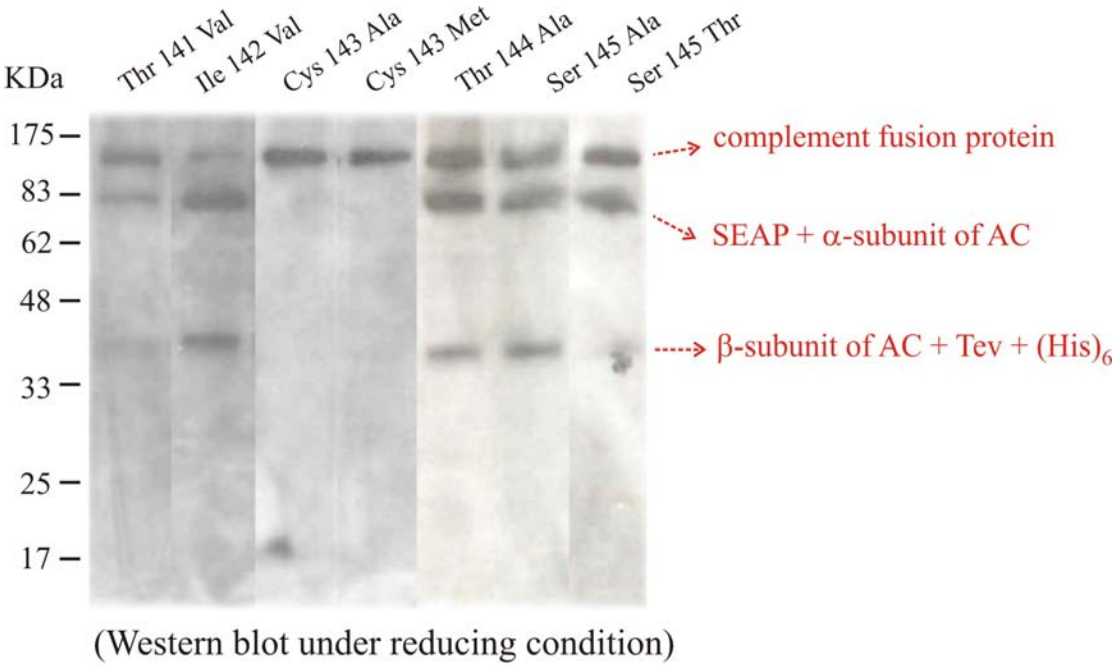

Fig. 2-7: Expressing a series of mutant fusion protein in baculovirus-infected Sf9 cells and then the culture supernatant was harvested at 3 days. 30 µl samples were loaded onto each lane of 8% Tris/Tricine SDS-PAGE gel and analyzed by Western blot.

It became clear that only mutants of the nucleophilic Cys, Cys143Ala and Cys143Met, do not show any proteolytic cleavage, whereas all other variants were still cleaved. We verified the expression of the mutant Cys143Ala again to determinate, whether the mutation delayed or completely blocked acid ceramidase proteolytic processing. No increase in α- or β-subunit was observed (Fig.2-8).

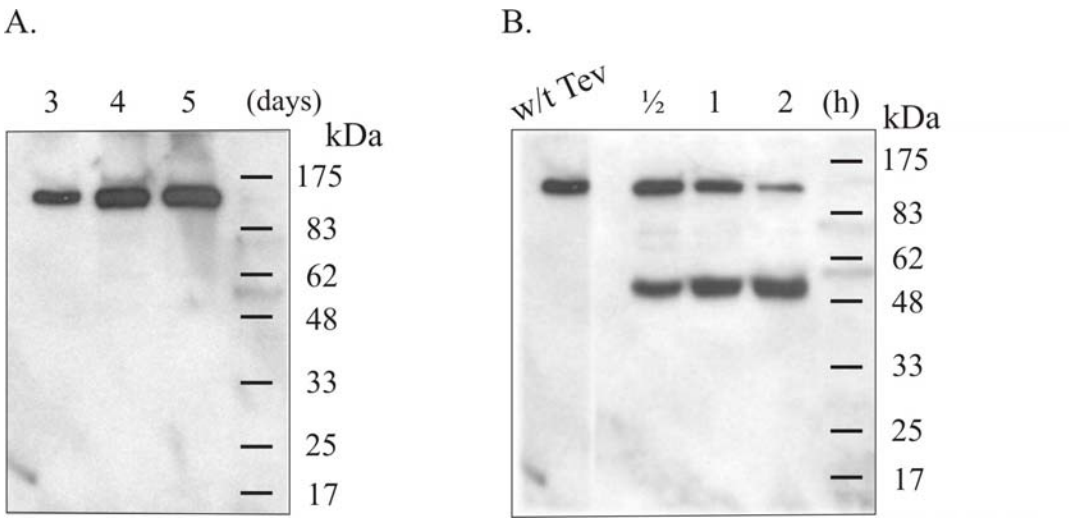

Fig. 2-8: Western blot with acid ceramidase antibody under reducing condition. (A.) Expression of the variant fusion protein (Cys143Ala) in baculovirus-infected Sf9 cells. The culture supernatant was collected at 3, 4, and 5 days, respectively. (B.) The supernatant including mutant fusion protein was digested with Tev protease in time-course.

Depending on this result, we assumed that Cys143, the N-terminal amino acid of the β-subunit of acid ceramidase, plays an important role in the maturation of acid ceramidase. Following this procedure, we can stop proteolytic processing of acid ceramidase, and then isolate a pure variant precursor of acid ceramidase for structural studies.

2.4 Purification and characterization of acid ceramidase precursor

2.4.1 Establishing the purification strategy for sufficient amounts of acid ceramidase precursor

For preparative expression and purification of variant fusion protein (Cys143Ala), stably transformed Sf9 cells were cultured as 800 mL suspension cultures in 2 L flask to a final density of 2.2 x 10^6 cells/mL. Since the expression level reached an approximate plateau after 96 hours, at this

time point, the medium was harvested by centrifugation (6000 rpm, 30 min) and kept at 4°C. As Fig.2-9 showed, the supernatant was then concentrated 10-fold by VivaFlow 200 (Vivascience) with filter-membrane 100,000 MW (PES), and then the concentrated medium was exchanged to DEAE-Sepharose equilibration buffer (50 mM Tris/HCl; 100 mM NaCl, pH 7.4) by dialysis overnight. The buffer-exchanged supernatant (200 ml) was then loaded onto DEAE-Sepharose (75 ml bed volume, Sigma) pre-equilibrated with washbuffer (50 mM Tris-HCl, 100 mM NaCl, pH 7.4). The suspension of flow-through was collected. After overnight dialysis with Ni-NTA washbuffer (50 mM NaH_2PO_4, 300 mM NaCl, 20 mM imidazole, pH 7.8), the suspension was clarified by centrifugation (10000 rpm, 30 min) and sterile filtration (0.2 μm). The filtrate was loaded onto a Ni-NTA superflow column (15 ml bed volume, Qiagen). After the column was washed with 40 ml of Ni-NTA washbuffer, absorbed proteins were directly eluted in 20 ml of 50 mM NaH_2PO_4, 300 mM NaCl, 125 mM imidazole (pH 7.8) elution buffer. The eluted sample was then concentrated 5-fold by Vivaspin 20 concentrater (Vivascience) with filter-membrane 100,000 MW (PES), 2000 rpm, and then the concentrated sample (final volume:~2 ml) was loaded onto gel fitration column: Superdex 75 Hiload 16/60 in FPLC system. Pooled fusion protein “SEAP-haCerasemut” fractions (Number:14~19.) were concentrated (final volume: ~2 ml) and buffer exchange with Tev-buffer (50 mM Tris/HCl, pH 7.6, 0.5 mM EDTA, 1 mM DTT) using Vivaspin 20 (Vivascience). Tev protease cleavage reaction was performed three hours at room temperature (Invitrogen). The digested sample was loaded again onto the same gel fitration column: Superdex 75 Hiload 16/60 in FPLC system. The newly appearing peak fractions were collected, resulting only in the purified enzyme ”haCerase” without SEAP and 6x histidine amino acids.

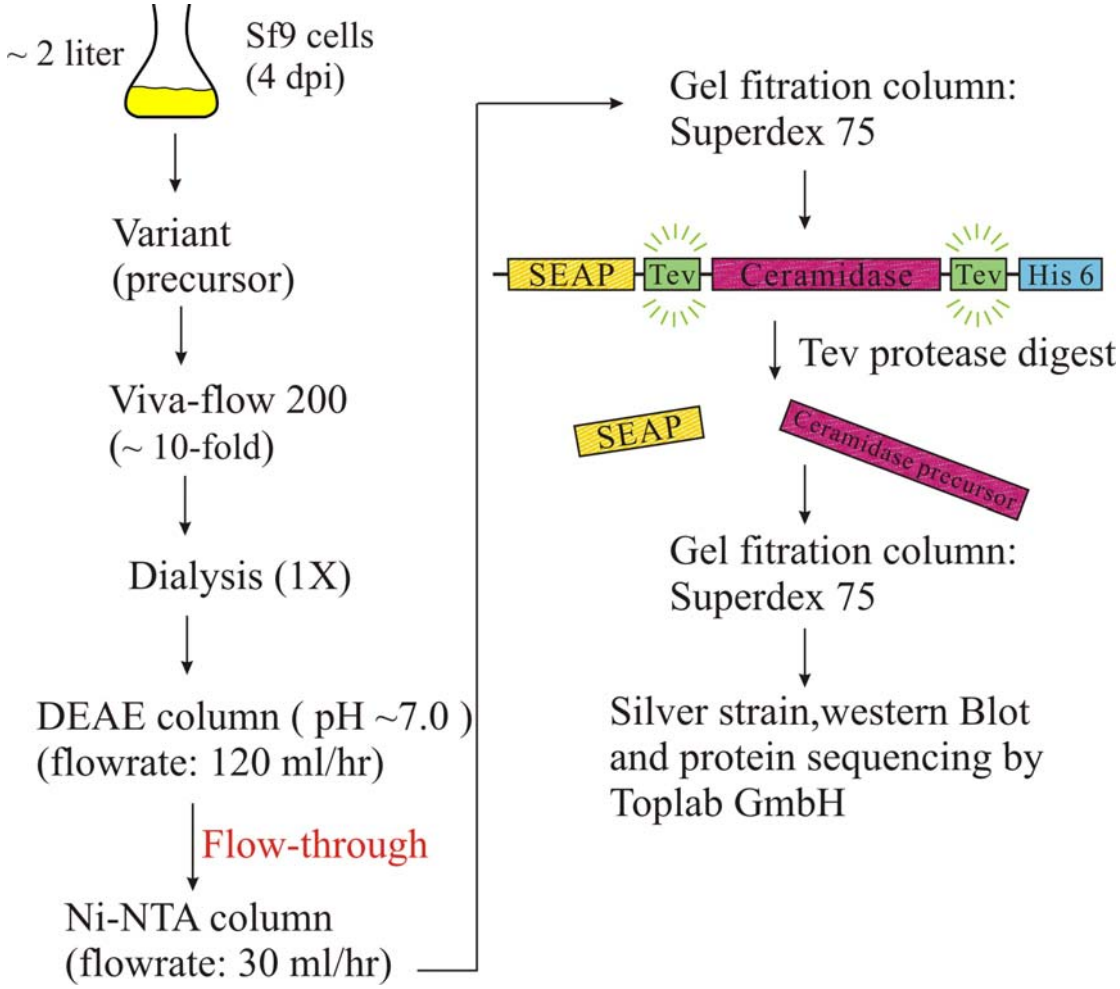

Fig. 2-9: Schematic illustration of the acid ceramidase precursor purification steps.

The purified precursor revealed a pure protein band around ~53 kDa as analyzed by SDS-PAGE followed by silver-staining. (Fig.2-10) and protein sequencing (Toplab GmbH). The purified acid ceramidase precursor (~80 μg pro liter culture medium) is currently used in crystallization experiments.

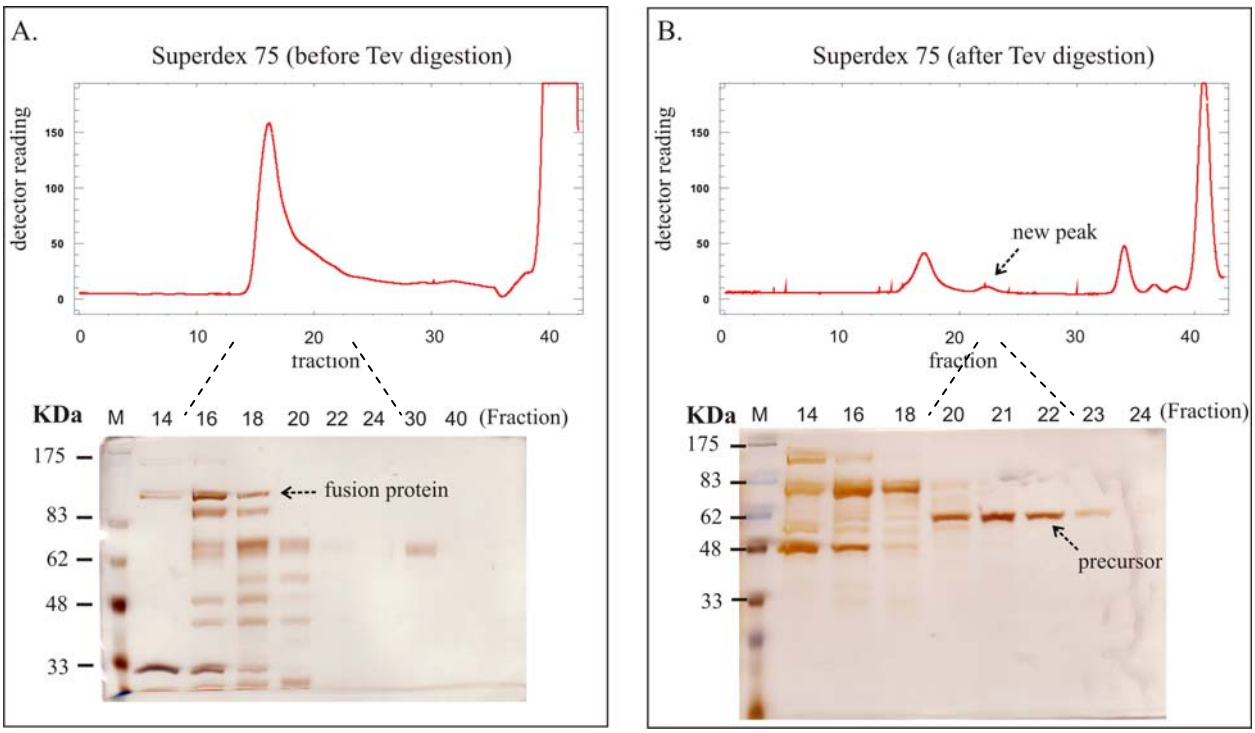

Fig. 2-10: Gel filtration: superdex 75 chromatography of fusion protein ”SEAP-haCerasemut” and then SDS-PAGE analysis. 30 µl of each fraction were loaded onto 8% Tris/Tricine SDS-PAGE under reducing condition. Proteins were then visualized by silver staining. (A.): The first running of gel filtration without Tev protease reaction. (B.): The second running of gel filtration after Tev protease digestion.

2.4.2 Activity analysis of acid ceramidase precursor

To further examine the influence of amino acid substitution (Cys143Ala) on ceramide-hydrolyzing activity of recombinant human acid ceramidase, both wild-type mature form and precursor (Cys143Ala) were allowed to react with N-lauroyl-sphingosine (C12-ceramide) in a micellar, detergent-based assay system (Bernardo *et al*., 1995). (Fig.2-11). Compared to wild-type the precursor (C143A) ceramidase had almost no activity, suggesting that Cys143 residue was also important for ceramide hydrolysis.

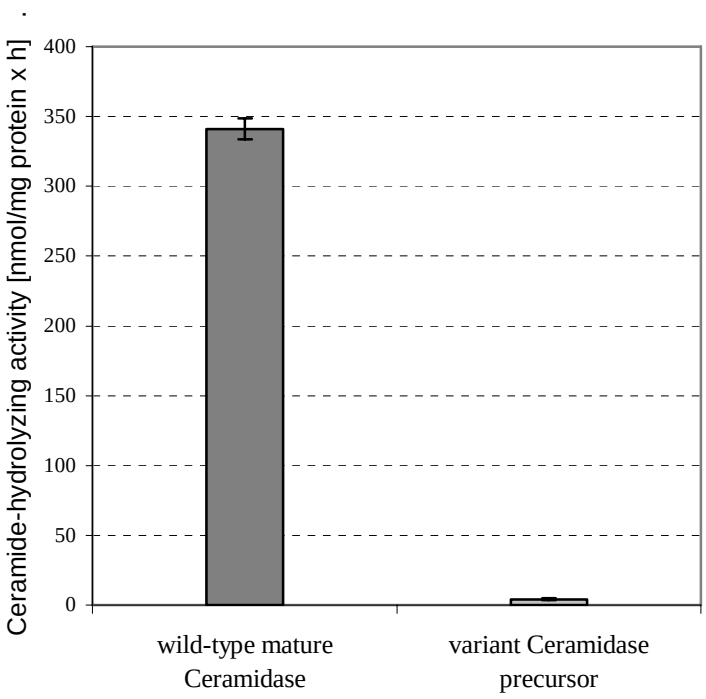

Fig. 2-11: Effect of Cys143Ala mutation on acid ceramidase activity.

2.5 Investigating the function of Cys143 in precursor processing mechanism

2.5.1 Inhibition studies of acid ceramidase proteolytic processing with p-chloromercuribenzoic acid

It has been shown that NAAA as described in the Introduction show similar processing activites as the ceramidase. When incubated at pH 4.5, the 48-kDa form of NAAA was time-dependently converted to the 30-kDa form with concomitant increase in the N-palmitoylethanolamine-hydrolyzing activity. The purified 48-kDa form was also cleaved and activated. However, the cleavage did not proceed at pH 7.4 or in the presence of p-chloromercuribenzoic acid (PCMB). The mutant Cys126Ser was resistant to the cleavage and remained inactive. These results suggested that this specific proteolysis is a self-catalyzed activation step.

It can be assumed that acid ceramidase catalyzes a similar reaction sequence at pH 4.0. The active center of acid ceramidase must therefore provide a nucleophile that reacts with the acyl carbon, an "oxyanion hole" that stabilizes the tetrahedral intermediate and an acid-base pair that transfers a proton to the leaving group sphingosine.

In order to find out which types of amino acids are possibly involved in ceramide degradation, acid ceramidase was incubated with a number of different group-specific inhibitors at pH 4.0 in previous studies of T. Linke (Linke 2000). Residual pAC activity was determined in a micellar assay system. The table shows that low concentrations of inhibitors directed toward cysteine and methionine dramatically decreased ceramidase activity activity.

		Concentration (μM) Residual enzymatic activity (in % of control)			
Inhibitor	**Specificity**	**0**	**1**	**10**	**100**
Thimerosal	Cysteine,	100	60	12	8
Iodoacetamide	Cysteine, Methionine	100	10	9	6
Phenylmethylsulfonyl fluorid (PMSF)	Serine	100	94	90	80
Ethyldiisopropylcarbodiimid (EDC)	Aspartate, Glutamate	100	60	25	10
Diethylpyrocarbonate (DPC)	Histidine	100	90	50	12

*Ceramide degradation was measured with purified protein in a detergent-containing, micellar assay system (From (Linke 2000))

The effect of the reducing agents, DTT and TCEP, were also tested at pH 4.0. Unexpectedly, treatment of ceramidase with TCEP at pH 4.0 increased enzymatic activity 3-fold, treatment with DTT at pH 4.0 1.5-fold (Linke 2000).

However, it is not clear whether this increase was due to a reduction of disulfide bonds. It is conceivable that other amino acids such as methionine or cystein became oxidised during the purification procedure of acid ceramidase. (Linke 2000)

In analogy to NAAA we already know that Cys143-substitution can not only stop the processing of the acid ceramidase precursor into mature form but also block the activity of acid ceramidase enzyme, suggesting that Cys143 residue was important. This result raises an interesting question as to whether Cys143 from (wild-type) acid ceramidase is free for enzymatic reaction or it is only involved in a disulfide-bridge for structural stabilization proposed by (Schulze et al. 2007). In this regard, it will be of particular interest to determine whether Cys143 can be modified by chemical cross-linker p-chloromercuribenzoic acid (pCMB). p-chloromercuribenzoic acid (pCMB) is an organic mecurial used as a sulfhydryl reagent. If Cys143 is indeed free and not involved in a disulfide bridge, it's thiol group could supposedly be modified with pCMB. Subsequently, as previously described, if Cys143 is modified, proteolytic processing of acid ceramidase should be prevented. According to this supposition, the Sf9 cells suspension culture were treated with pCMB (final conc. 1mM) after 3 days of infection Fig.2-11 Western blotting analysis further revealed that wild-type fusion protein "SEAP-haCerase" with 1 mM pCMB completely inhibited processing of acid ceramidase. After pCMB was added to the infected Sf9 cells suspension culture including acid ceramidase, maturation of the ceramidase into α- and β- subunits was prevented and only the processing product, which was already present before the pCMB treatment, was detected.

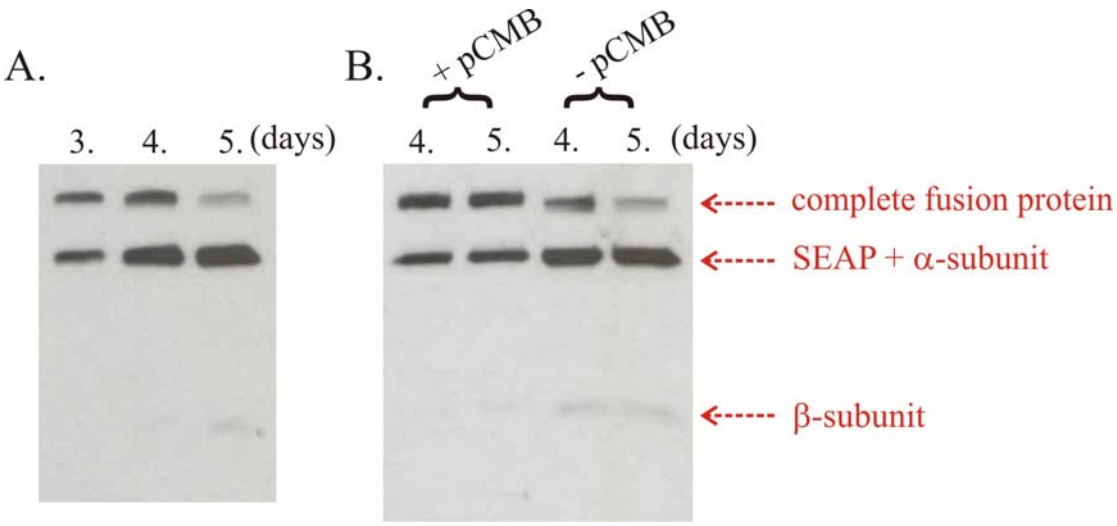

Fig. 2-11: Inhibition of acid ceramidase proteolytic processing with pCMB. (A.) As control: without pCMB treatment in infected Sf9 cell suspension. (B.) After 3 days infection, the infected Sf9 cell suspension was treated with/without pCMB. Expressing wild-type fusion protein in baculovirus-infected Sf9 cells and then the culture supernatant was collected at 3, 4, and 5 days, respectively, and analyzed by SDS-PAGE followed by Western blot using acid ceramidase antibody.

2.5.2 Identifying Cys143 of acid ceramidase as marked residue by pCMB

pCMB prevented the processing of the ceramidase precursor into its mature form. Cys143 should contain a free thiol function, which could be labeled by pCMB. For further determination, whether Cys143 of acid ceramidase was labeled with pCMB, the treated acid ceramidase was “In-gel” digested with trypsin protease and the resulting products were analyzed by MALDI-MS for peptide containing modified or not modified Cys residue.

The In-gel digestion protocol was originally introduced in 1996 by Shevchenko et al. (Shevchenko et al. 2006), and has been used thousands of times over the last 10 years. The In-gel digestion procedure is compatible with down-stream mass characterization of digests of isolated protein band. MALDI-MS Identification of proteins from In-gel digestion offers some important advantages compared to In-solution digestion. For example, gel

electrophoresis removes low molecular weight impurities, including detergents and buffer components, which are often detrimental for mass spectrometric sequencing. Use of pure protein (single band) for mass spectrometric analysis, decreases a significant background noise of digested products.

The pCMB-treated Sf9 cell culture supernatant was harvested 4 days post-infection, acid ceramidase was then purified. After first gel-filtration column: superdex-75 purification step, the concentrated sample (~0.8 mg) was loaded onto 8% Tris/Tricine SDS-PAGE under reducing condition, excising the band of fusion protein “SEAP-haCerase”, In-gel trypsin digestion according to manufacture’s protocol (Andrej et al., 2007), prior to MALDI-MS identification of peptide containing pCMB labeled Cys143. To analyze the result of In-gel trypsin digestion, Fig.2-12 shows the tryptic peptides of the acid ceramidase precursor after trypsin digestion.

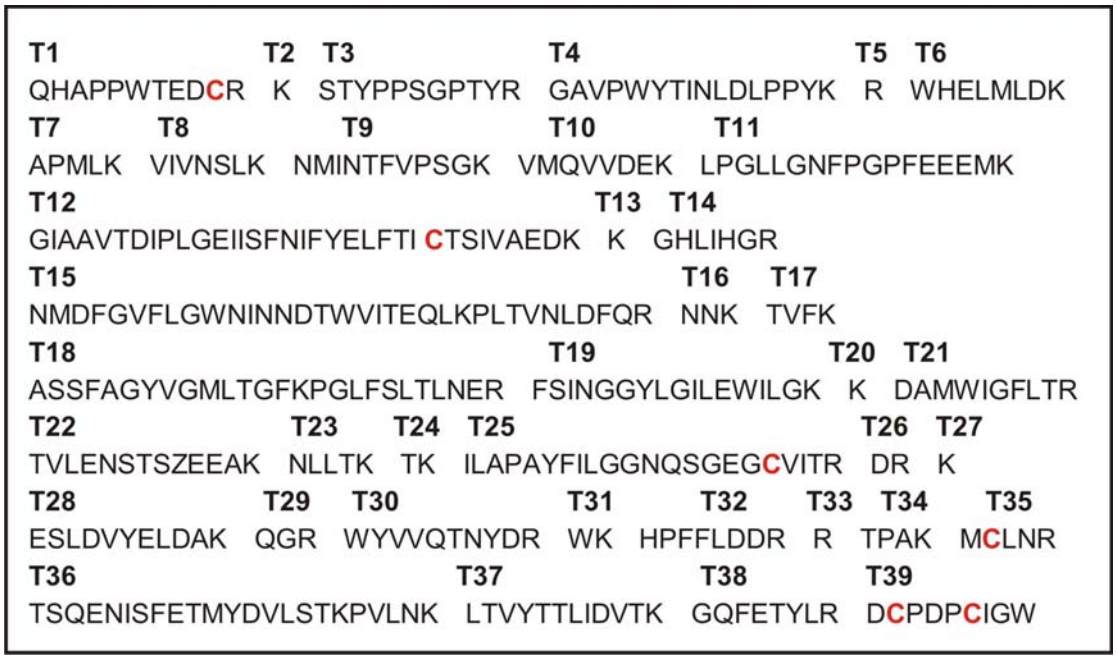

Fig. 2-12: Amino acid sequence of the acid ceramidase precursor. Tryptic cleavage sites are indicated by gaps, tryptic peptides are named T und numbered from 1 to 39. Cysteine residue was labeled in red (Adapted from (Schulze et al. 2007)) The tryptic cleavage pattern was generated using the Swissprot database.

The resulting In gel digestion peptides were identified as tryptic peptides by their mass. Based on Fig.2-12, instead of the wild-type Cys143-peptide “T12” with a mass of 3704 Da, the mass of mutant Cys143Ala-peptide “T12” should be 3672 Da. The peptide containing the pCMB-labeled Cys143 residue has a mass that is increased by 322 Da (mass of pCMB) compared to the untreated Cys143-peptide. As shown in Fig.2-13 in the MALDI spectrum detected peptides, we did not find any significant peak corresponding to untreated Cys143- or pCMB-labeled tryptic peptide “T12”. Excluding peptide recovery from gel as shown above, the main reason for this may be that long peptide still remains trapped in the gel due to poor diffusion or the crosslinkt peptide is not sufficiently digested.

A.

untreated mutant precursor:
calculated mass:
Peptide “T12”: 3672 Da

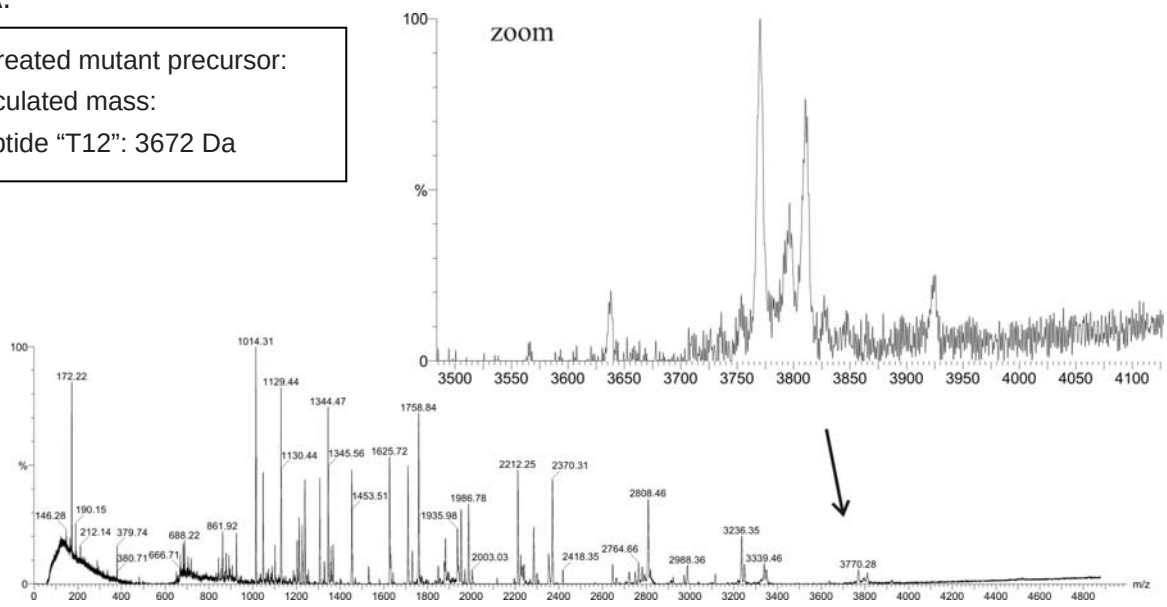

B.

pCMB-treated wild-type acid ceramidase:
calculated mass:
unlabeled peptide “T12”: 3704 Da
pCMB-labeled “T12”: 4026 Da

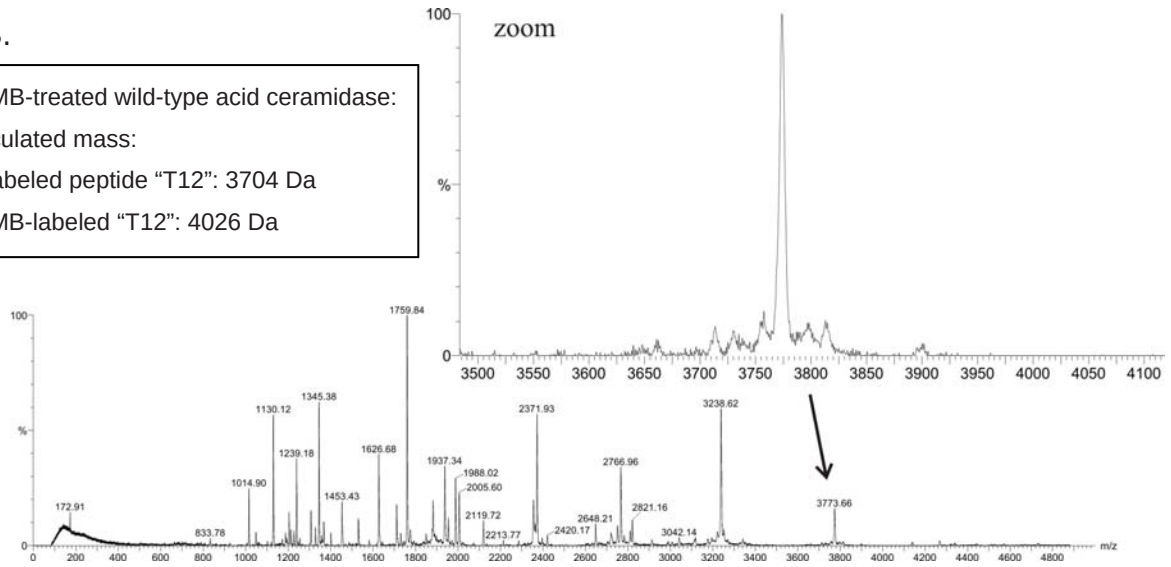

Fig. 2-13: MALDI Mass spectrum of the tryptic digest and the corresponding inset zoom scan of the Cys143-peptide “T12”. (A.) Untreated mutant fusion protein “SEAP-haCerase”. (B.) pCMB treated wild-type fusion protein “SEAP-haCerase”.

Unfortunately, there is no direct evidence to demonstrate whether the Cys143 residue is free, but some indirect data were still obtained from MALDI-MS analysis. Perhaps due to better diffusion efficiency of small peptides from gel, MALDI Mass spectrometry resulted in high yield of small peptides that occurred after In gel trypsin digestion. According to the previous published results (Schulze, 2007), there is a disulfide bond that occurred between Cys143 and Cys292. If Cys143 of acid ceramidase was free, the other cysteine residue: Cys292 of acid ceramidase should be also in a free state. Base on Fig.2.12, the tryptic peptide containing Cys292 is “T25” peptide that has a mass of 2280 Da. On the other hand, the peptide containing the pCMB-labeled Cys292 residue should have a mass that is increased by 322 Da to the mass of 2602 Da. As shown in Fig.2-14. (B.), after pCMB treatment of the wild-type SEAP ceramidase fusion protein the spectrum showed that the peptide corresponding to the Cys292-peptide “T25” has a significant decrease

in the peak compared to untreated fusion protein. At the same time, a new signal was obtained. However, the signal for this peptide corresponding to the correct mass was weak, but detectable. Therefore, Cys292 residue should be probably at least partially in a free state. According to this indirect evidence above, the Cys143 residue should be also in a free state.

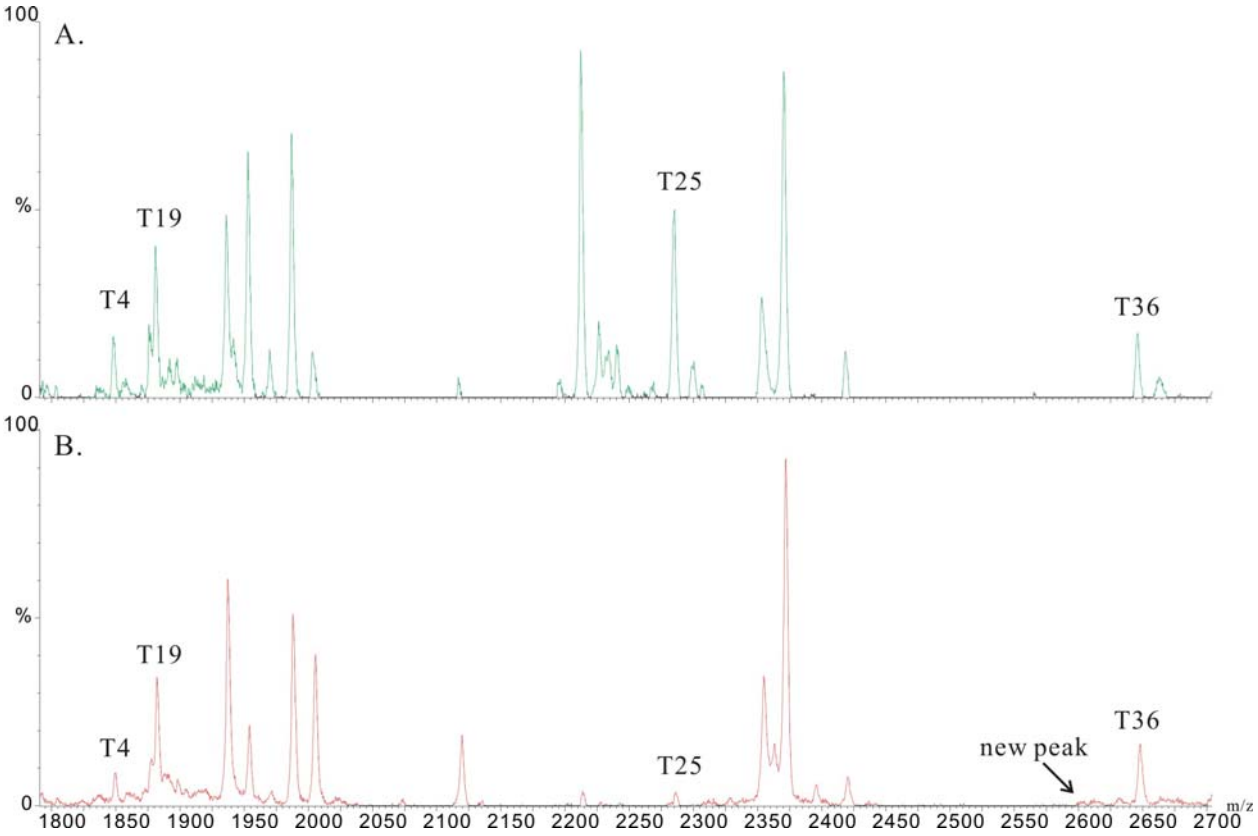

Fig. 2-14: MALDI Mass spectrum of the corresponding inset zoom scan of the Cys292-peptide “T25” and some of the other tryptic peptides from acid ceramidase. (A.) Untreated mutant fusion protein “SEAP-haCerase”. (B.) pCMB treated wild-type fusion protein “SEAP-haCerase”.

2.6 Cross-linking experiment between acid ceramidase and saposin D

The ceramide hydrolysis by acid ceramidase *in vivo* requires the presence of saposin D (Klein et al. 1994), but it is still unclear whether Sap D and acid ceramidase have *in vivo* protein-protein interaction domains. In order to demonstrate whether a binding or affinity domain between acid ceramidase and Sap D exists, cross-linking interaction experiments in cells between Sap-D and acid ceramidase were studied.

2.6.1 *In vivo* cross-linking experiment

Cross-linking is a useful tool in the study of protein-protein reactions, but the nature of most cross-linking methods prevents their use in live cells. Recently, the use of photo-reactive amino acid analogs to create cross-links between interacting proteins has allowed to study protein complexes *in vivo*. Analogs of leucine and methionine, both featuring photosensitive diazirine rings, are fed to growing cells. These analogs are incorporated into proteins and create cross-links between interacting proteins when exposed to ultraviolet light.

Photo-sensitizers undergo photo-excitation with exposure to light, transferring energy to reactions. The photo-excited molecules are generally very reactive as well, frequently binding readily to nearby compounds. The amino acid analogs, such as the one used in the following experiments, take advantage of the reactivity of photo-excited molecules. The analogs are identical to the natural amino acids, except for a photosensitive diazirine ring. When exposed to UV light, the nitrogen is released and a reactive carbene is formed.

The activated carbene has a very short half-life, so reactions must occur with groups in a very close proximity. In a protein complex, the carbenes will react with nearby groups to form stable cross-links that “freeze” the complex in its current position, allowing to analyze the protein-protein interactions within the complex.

L-photo-leucine is an analog of L-leucine amino acid. It contains a diazirine ring for crosslinking with ultraviolet light (UV) and can substitute *in vivo* natural amino acid (L-leucine) into primary sequence of proteins during synthesis (Fig.2-15).

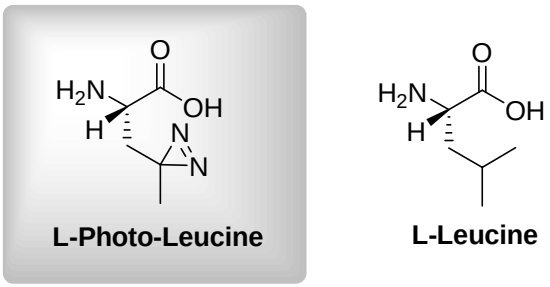

Fig.2-15: Structure of L-Photo-Leucine containing a diazirine cross-linking unit and it's natural analog.

The photoleucine is used in combination with Dulbecco's Modified Eagle's limiting media that is devoid of leucine and methionine, As a result, L-photo-leucine can be substituted for leucine in the primary sequence of proteins. Crosslinked protein complexes can then be detected by running SDS-PAGE followed by Western blot (Fig.2-16).

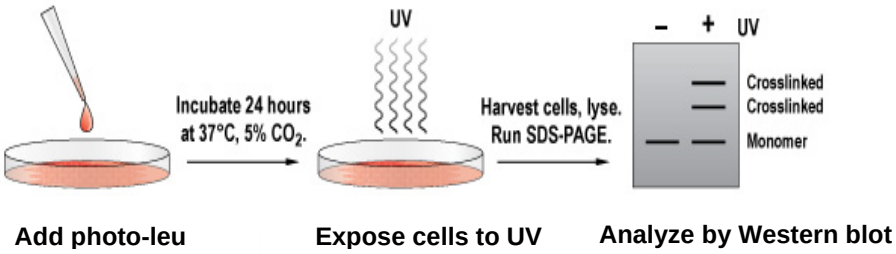

Fig.2-16: Protocol summary for protein interaction experiments with L-Photo-Leucine in baby hamster kidney (BHK) cells.

To probe for for interaction of acid ceramidase and Sap-D with photo-leucine, different cell lines such as HeLa cells, human primary fibroblasts and baby hamster kidney cells (BHK) overexpressing prosaposin or Sap-precursor, were incubated with the leucine deficient medium. The cells were incubated for 24h

and the medium was discarded. The cells were washed with PBS and irradiated with UV light, they were harvested and lyzed in RIPA buffer. Likewise, the same set of cells treated with 1% paraformaldehyde (PFA) for 30 min for PFA-crosslinking. The cells were harvested and also lyzed in RIPA buffer. Eventually, the lysates were analyzed by SDS-PAGE and simultaneaous Western blots with goat anti-Sap-D and rabbit anti-ceramidase antibodies

As shown in Fig.2-17, the result suggests that the same band (as red arrow between 83 and 62 kDa) was detected both with Sap-D and acid ceramidase antibody. Further analyses suggested the interaction site within the α-subunit of the ceramidase. However these results need to be verified by other crosslink experiments

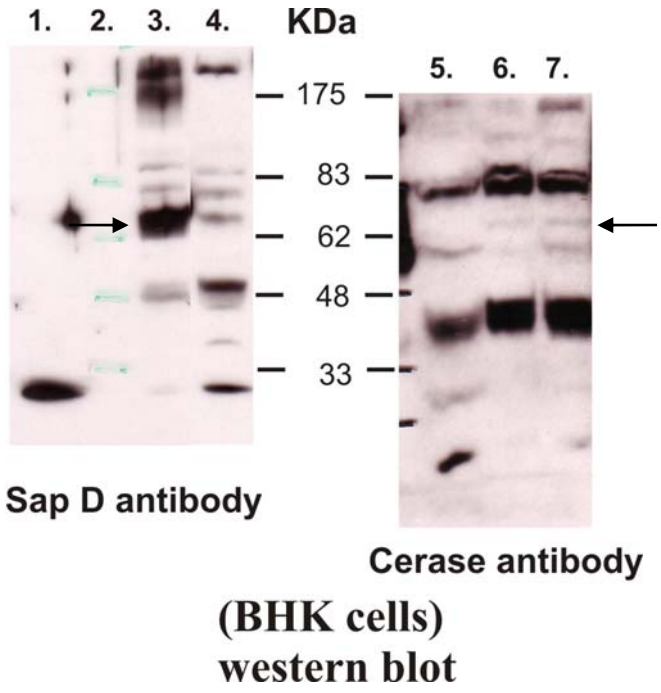

Fig.2-17: Direct protein interaction analysis of the *in vivo* crosslinking experiments of acid ceramidase and Sap D. BHK cells lysates (10 μg) were loaded onto each lane of 8% SDS-PAGE followed by western blot to detect cross-links with Sap D antibody or Ceramidase antibody. Lane1: purified Sap D as control. Lane2: standard protein marker. Lane3, 6: cells were treated with photo-leucine followed by UV treatment. Lane4, 5: cells were untreated. Lane7: cells were treated with 1% paraformaldehyde (PFA) on ice for 30 min.

2.6.2 *In vitro* cross-linking experiment

In analogy to the *in vivo* experiments, *in vitro* crosslink experiments with purified acid ceramidase and Sap-D were performed. Here we used a very common bifunctional crosslink reagent. DSG (Disuccinimidyl glutarate) (Fig.2-18) is a homobifunctional *N*-hydroxysuccinimide ester (NHS-ester). Primary amine from lysine side chains is a principal target for NHS-esters. A covalent amide bond is formed when the DSG reacts with primary amines of protein. This cross-linker is noncleavable, even when analyzed by SDS PAGE under reducing condition.

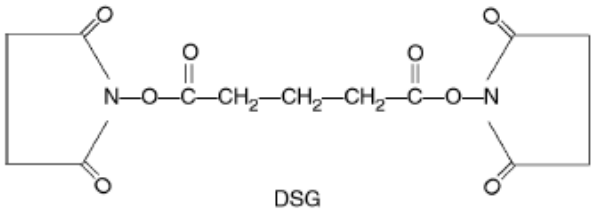

Fig.2-18: Structure of DSG.

The purified wild-type and mature acid ceramidase and purified unglycosylated recombinant Sap-D were mixed in reaction buffer followed by treatment with DSG. After SDS-PAGE the crosslinked mixture was analyzed by Western blot using rabbit anti-acid ceramidase antibody or goat anti-Sap D antibody, as shown in Fig.2-19. The experiment revealed the cross-link product band at the same molecular weight (between 83 and 62 kDa) as found in the *in vivo* cross-linking test. The predicted molecular weight of a cross-link between one monomer of Sap-D and one monomer of ceramidase would be around 65 kDa. As there are also cross-link bands around 120 kDa one would assume an interaction between Sap-D dimer and a ceramidase dimer. The mass spectrometry of these cross-link products is ongoing and so far we cannot predict the correct composition of these bands.

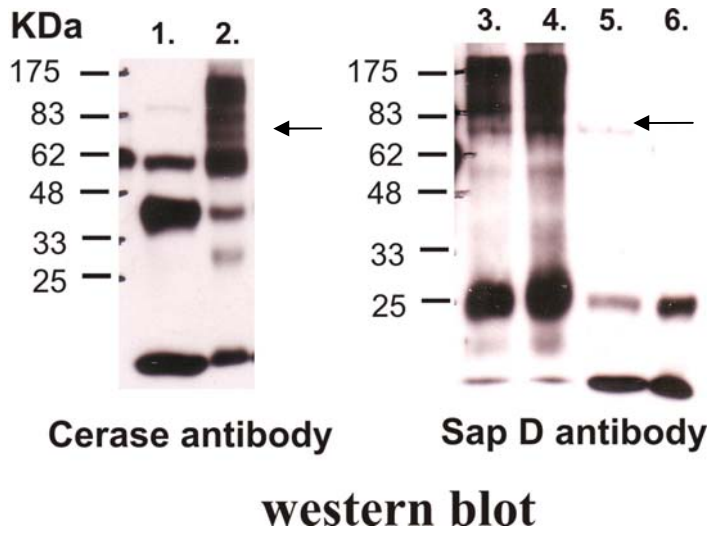

Fig. 2-19: The purified protein interaction test *in vitro* between acid ceramidase and Sap D. After DSG treatment at room temperature for 30 min, or in the absence of DSG, the samples (20 μl) were analyzed by SDS-PAGE followed by western blot to detect cross-links with ceramidase antibody or Sap D antibody. Lane1: Only purified acid ceramidase untreated with DSG. Lane2, 3: acid ceramidase and Sap D protein mixture (1:1) treated with DSG. Lane4: acid ceramidase and Sap D protein mixture (1:2) treated with DSG. Lane5: acid ceramidase and Sap D protein mixture (1:1) not treated with DSG. Lane6: Purified Sap-D treated with DSG.

As shown in Fig. 2-20, unglycosylated Sap-D from recombinant expression could be mainly purified as a homodimer and a monomer. The same seems to be the case for the ceramidase in some experiments we could detect a cross-link product of an α-homodimer and a dimer of the mature ceramidase. Fig. 2-20 also shows Sap-D and ceramidase cross-link products in a range of about 62-150 kDa suggesting a cross-linking between monomers or dimers of both.

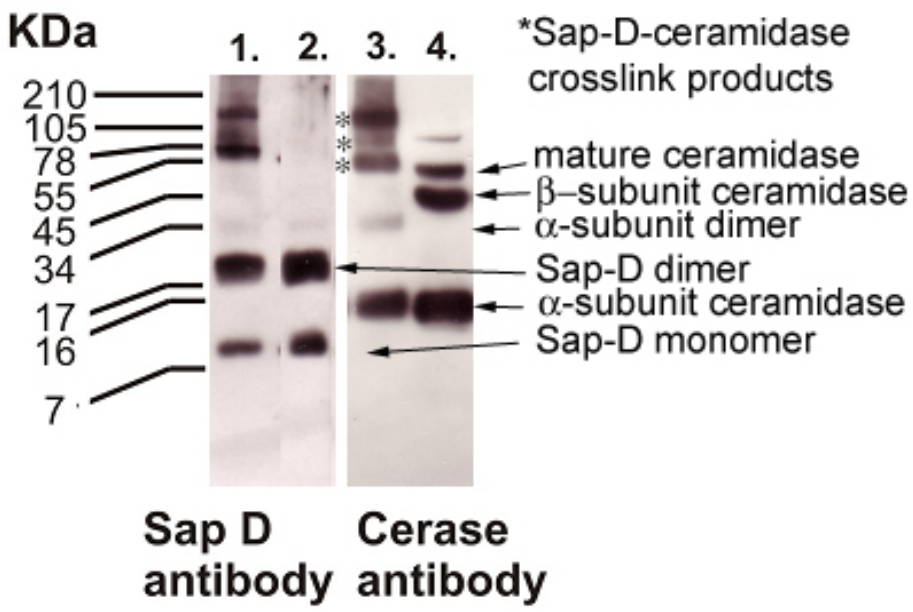

Fig. 2-20: The purified protein interaction test *in vitro* between acid ceramidase and Sap D. After DSG treatment at room temperature for 30 min, or in the absence of DSG, the samples (20 µl) were analyzed by SDS-PAGE followed by western blot to detect cross-links with ceramidase antibody or Sap D antibody. Lane1: Acid ceramidase and Sap D protein mixture (1:2) treated with DSG. Detection with anti Sap-D antibody. Lane 2: Purified Sap-D treated with DSG Lane Detection with anti Sap-D antibody. Lane 3: Acid ceramidase and Sap D protein mixture (1:2) treated with DSG. Detection with anti ceramidase antibody. Lane4: Only purified acid ceramidase untreated with DSG. The cross-link products are assumed to correspond to the indicated protein forms.

In a further experiment, the influence of lipids such as ceramide and bismonoacylglycerophosphate (BMP) on the binding of Sap-D and ceramidase was investigated (Fig. 2-21). Unfortunately, we could not detect any effects since the binding assay does not seem compatible with the cross-linking conditions. Sap-D seems to be dislocated from the ceramidase since no crosslink products can be detected. It can be assumed that Sap-D is depleted by the liposomes as it is unglycosylated and hydrophobic.

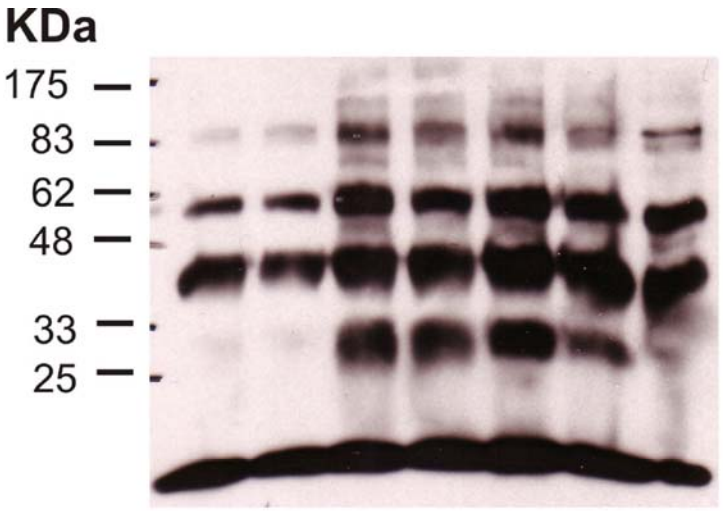

sap D and cerase mixture (1:1)	+	+	+	+			
only acid ceramidase					+	+	+
Liposome: pc/chol/BMP/cer 12	+	-	+	-	+	-	-
DSG	-	-	+	+	+	+	-

Fig. 2-21 DSG Cross-linking experiments of ceramidase and Sap-D in presence or absence of lipids. The detection was performed with anti-ceramidase antibody

3 Discussion

3.1 Expression and Characterization of recombinant fusion protein "SEAP-haCeramidase"

The main goal of this study was the expression of recombinant human acid ceramidase precursor in insect cells (Sf9) to yield sufficient amounts of homogeneous enzyme for biophysical and structural investigations. We have already expressed human acid ceramidase in insect cells (Schulze et al. 2007), but the separation of precursor and mature acid ceramidase obtained from the culture supernatant of the Sf9 cells was very difficult and could only be achieved under denaturating conditions. In order to generate the recombinant baculovirus expressing only the human acid ceramidase precursor, a fusion construct of secretory alkaline phosphatase (SEAP) - Tev cleavage site - acid ceramidase (preprotein) - Tev cleavage site – 6xHis tag was designed. With the help of SEAP, the infected Sf9 cells quickly secreted a fusion protein "SEAP-haCerase" into the medium to avoid proteolytic processing of acid ceramidase. For this purpose the different genetic building blocks were amplified in several PCRs. The PCR products: "SEAP-Tev" and "haCerase-Tev-6xHis" fragments were ligated into the pFastBac transfer vector. The recombinant plasmid was transposed into the baculo genome, which was used to generate a recombinant virus. Following the infection of Sf9 cells with the recombinant virus "SEAP-haCerase" was successfully synthesized as a 110 kDa fusion protein. However, proteolytic processing into its heterodimeric mature form (40 kDa and 70 kDa) still occurred in the medium despite the help of SEAP, which should prevent the processing by only expressing the secreted ceramidase.

3.2 Expression and Characterization of mutant fusion protein "SEAP-haCeramidase"

Initially, we assumed that proteolytic processing of acid ceramidase would be achieved presumably by a lysosomal protease, which might be active in Sf9 cell culture supernatant and was acting as a "substrate-proteinase" (Carrington et al. 1988). For example, the proteinase can require a specific sequence motif at the cleavage sites for correct recognition of the substrate. If the ceramidase cleavage motif would be changed, the proteolytical cleavage should be impaired. According to this supposition, we have made point mutations to alter the amino acids near the cleavage site to avoid proteolytic processing of acid ceramidase.

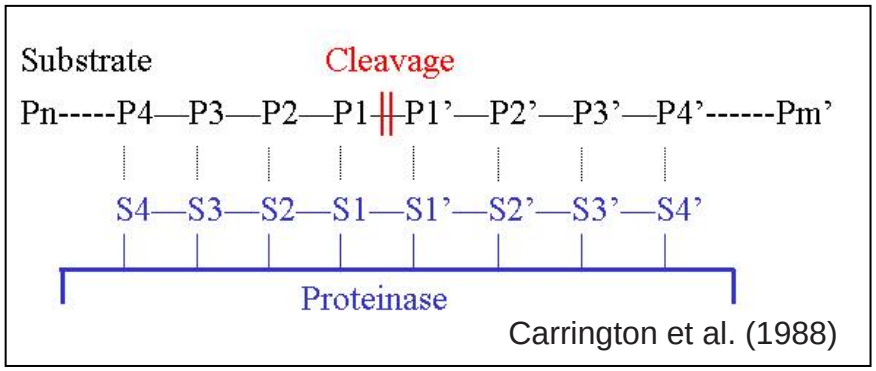

Carrington et al. (1988)

Seven mutants were engineered by substituting the residues with different amino acids (Thr141, Ile142val, Cys143Ala, Cys143Met, Thr144Ala, Ser145Ala, Ser145Thr). But the result did not correspond to our theory, as shown in Fig.2-7, It became clear that only the variant ceramidase, which contain an exchange of the nucleophilic Cys to Cys143Ala and Cys143Met is impaired in proteolytic cleavage, whereas all other variants were still cleaved. Therefore, proteolytic processing of acid ceramidase was assumed to occur autocatalytically into its α- and β- subunits, similar to other members of the N-terminal nucleophile (Ntn) hydrolase superfamily.

As only the substitution of nucleophilic Cys143 does not show any proteolytic cleavage, we established the overexpression and purification of the variant Cys143Ala fusion protein to produce a large amount of acid ceramidase

precursor, in order to analyze the structure in crystallization experiments. By crystallographic studies of the precursor and the mature ceramidase, we can obtain detailed insights into the structures, catalytic center, and the complete cleavage mechanism of ceramidase.

3.3 The investigation into the function of Cys143 in acid ceramidase

As described above, the proteolytic processing of acid ceramidase seems to reveal an α- and a β- subunits. In addition, we already know that Cys143-substitution (be meant also as modification) can not only stop the processing of the acid ceramidase precursor into its mature form but also blocked the activity of acid ceramidase enzymatic function, suggesting that Cys143 residue plays a critical role in acid ceramidase activity. More importantly, using extensive sequence similarity searches (Altschul et al. 1997), acid ceramidase is homologous to lysosomal N-acylethanolamine hydrolyzing acid amidase (NAAA) and penicillin V acylases (PVA) (Tsuboi et al. 2007), which belong to the superfamily of N-terminal nucleophile (Ntn) hydrolases. According to these findings above, we propose that the acid ceramidase is also a member of Ntn-hydrolase superfamily .

There are a total of 6 cysteine residues among the primary sequence of acid ceramidase, all of the 6 cysteines might be involved in 3 different disulfide bonds for structural stabilization (Schulze et al. 2007), but based on the good inhibititory effect of iodoacetamide (IAA), a cysteine protease inhibitor, on acid ceramidase (Linke, 2000) , we presumed that at least one of six cysteines residues could be involved in the catalytic center of acid ceramidase. If acid ceramidase belongs to superfamily of Ntn-hydrolases, after cleavage, the N-terminal nucleophilic Cys143 of the β-subunit should serve as the active site for ceramide hydrolysis. Therefore, the Cys143 residue must at least partially contain a free thiol group. Consequently, when Cys143 will be labeled by

sulfhydryl reagent pCMB, proteolytic processing of acid ceramidase should be prevented. As shown in Fig.2-11, we confirmed that Cys143 residue should be in a free state. Although a MALDI MS spectrum for further demonstration failed to detect the pCMB labeled freagment, we still found some indirect evidences to support our concept (Fig.2-15). In addition, a model of the tertiary structure of the acid ceramidase β-subunit using the crystal structure of cholylglycine hydrolase, one member of the Ntn hydrolases, as a template (Shtraizent et al. 2008) revealed that Cys143 was too far from other cysteine residues, such as Cys292, to form a disulfide bond. According to the description above, we believe that Cys143 residue should contain at least partially a free thiol group not associated in a disulfide bond, which serves as catalytic site, although Schulze et published the existence of a disulfide bridge between Cys143 and Cys229 (Schulze et al., 2007). So far, we cannot exclude that to a partial extend such disulfide bridge exists or how much of the catalytic Cys143 is not involve in a disulfide bridge. Likewise, we cannot exclude whether purification of the recombinant proteins led to aging and oxidation of the cysteins and or building of the disulfide bridges. However, the fact that ceramidase, even more abundant than sphingomyelinase, is less active than sphingomyelinase might be due to only partially active protein, in which the majority of the Cys143 is involved in disulfide bridges. Nevertheless, in our preparation of the protein we could not detect any disulfide bridges.

3.4 Cross-linking experiment between acid ceramidase and Saposin D

The lysosomal degradation of ceramide is catalyzed by acid ceramidase and requires saposin activator protein D (Sap-D) as cofactors *in vivo*. To further investigate whether a binding domain exists between acid ceramidase and Sap-D *in vivo*, BHK cells overexpressing saposin precursor and subsequently Sap-D were treated by L-photo-leucine. A cross-linking protein complex between 83 and 62 kDa was detected by acid ceramidase antibody as well as

by Sap-D antibody. Likewise, the cross-linking test between purified acid ceramidase and purified Sap-D *in vitro*, the same band could be recovered. Depending on the standard protein marker, this cross-linking protein complex consisted of acid ceramidase and Sap-D in the ratio 1:1. Interestingly, Unglycosylated Sap-D from recombinant expression in Pichia pastoris shows a dimerization of Sap-D. For ceramidase one can detect a band corresponding to a dimer and a tetrameric form. According to the model of lipid activation by Sap-D (Rossmann et al. 2008), the dimer Sap-D extracts lipid molecule from the membrane. Perhaps more importantly, ceramidase could subsequently interact with the dimer Sap-D and lipid molecule due to our cross-linking result. The next step of the process is the hydrolysis of lipid molecule from the complex. With the help of Sap-D acting as the “solubilizer” (Ciaffoni et al. 2001), water-soluble ceramidase could more effectively degrade ceramides from the lipid bilayer.

4 Summary

Ceramides are important building blocks of eukaryotic membranes and primarily serve as membrane anchors of GSLs and sphingomyelins. The lysosomal degradation of ceramide is catalyzed by acid ceramidase and requires the interaction with Sap-D *in vivo.* Acid ceramidase is synthesized as a monomeric precursor followed by proteolytic processing into mature enzyme which is a heterodimer consisting of α- and β- subunits. The main goal of this study was to establish the recombinant expression in insect cells and purification of only the human acid ceramidase precursor for further crystallization studies. In order to generate the recombinant baculovirus expressing only the human acid ceramidase precursor, a fusion protein was constructed with SEAP. However, this strategy failed and proteolytic processing of acid ceramidase still occurred. Subsequently, the amino acids near the cleavage site were substituted by point mutation to avoid proteolytic processing. It only worked with the mutant of the nucleophilic Cys143, which did not show any proteolytic cleavage, whereas all other variants were still cleaved. Therefore, proteolytic processing of acid ceramidase seems to occur autocatalytically by self-cleavage into α- and β- subunits, similar to other members of the N-terminal nucleophile (Ntn) hydrolase superfamily. We established the overexpression and purification of the variant Cys143Ala fusion protein to produce a large amount of acid ceramidase precursor for further crystallization experiments.

Treatment of wild-type fusion protein “SEAP-haCerase” with the cysteine protease inhibitor, p-chloromercuribenzoic acid (pCMB), inhibited both self-cleavage and enzymatic activity. More importantly, Cys143 residue was also confirmed to be in a free state. Therefore, we suggest that acid ceramidase also belong to the superfamily of Ntn-hydrolases.

5 Material and Methods

5.1 Technical equipment and materials

5.1.1 Technical equipment

Technical equipment:	Specification/Manufacturer	City
Analytical HPLC LDP10$_{AT}$	Shimadzu	Duisburg
Autoclave	Systec	Wettenberg
Autosampler AS 200	Biorad	München
Blot apparatus Mini-Transblot	Biorad	München
Centrifuges Sorvall RC 5B	DuPont	Bad Homburg
Centrifuge rotors JA 10, Ti 80	Beckmann	München
Fluorescence detector RF 10$_{AX}$	Shimadzu	Duisburg
FPLC-System	Pharmacia Biosystem	Freiburg
Gel apparatus Mini-Protean ll	Biorad	München
Incubator	1083/Gesellschaft für Labortechnik	Burgwedel
Isothermal titration calorimeter	VP-ITC/ MicroCal	Amherst, USA
MALDI-MS TOF Spec E	Micromass	Mancheter, UK
Perstaltic pump P1	Pharmacia Biosystem	Freiburg
pH-meter pH 537	WTW	Weilsheim
Power supply : model 250/2.5	Biorad	München
Preparative HPLC Biocad Sprint	PE Biosystem	Weiterstadt
Table top centrifuges Modell 5412	Eppendorf	Hamburg
Thermomixer Comfort	Eppendorf	Hamburg
Thermocycler: PTC-200	MJ-Research/Biozym	Oldendorf
Ultrasonic irradiation system Sonifier 250	Branson	Danbury, USA
Ultraturrax TP 1810	Janke & Kunkel	Staufen
Votex	MS Minishaker/Ika-Werk	Staufen

Water filtration system Super Q	Millipore	Molsheim, France

5.1.2 Columns

Columns:	Specification/Manufucturer	City
Hiload XK26	Pharmacia Bioteck	Freiburg
LiChroCART 125-4 Nucleosil 5 C18	Merck	Darmstadt
Q-Sepharose Hiload 26/20	Pharmacia Bioteck	Freiburg
Superdex 75	Pharmacia Bioteck	Freiburg

5.1.3 Chemicals

Chemical:	Specification/Manufacturer	City
Acetic acid	Merck	Darmstadt
Acrylamide solution 29:1, 30%	Biorad	München
Alkaline phosphatase, conjugated to anti-goat lgG	Sigma	Deisenhofen
Ammoniumperoxodisulfate	Bioland	München
BCA solution	Sigma	Deosemjpfem
Buffer salts	Merck	Darmstadt
Ceramides	Matreya Lipids	Köln
Chloroform, p.a.	Fluka	Neu-Ulm
p-chloromercuribenzoic acid	Fluka	Neu-Ulm
Colloidal Coomassie Blue, Image Enhancer	ICN	Eschwege
Coomassie Blue G250	Serva	Herdelberg
DEAE sepharose	Sigma	Deisenhofen
Fluoroaldehyde	Pierce	Rockford, USA
β-Mercaptoethanol	Sigma	Deisenhofen

Methanol HPLC-grade	Riedel-de Haen	Seelze
Ni-NTA superflow	Qiagen	Hilden
PVDF membranes	Porablot, Macherey-Nagel	Dassel
Restriction-enzyme: Bam HI, Kpn I, Sal I, Bgl II	NEB	Schwalbach
SDS	Sigma	Deisenhofen
Silver nitrate	Merck	Darmstadt
Sodium cholate	Deisenhofen	Sigma
T4-DNA-Ligase	NEB	Schwalbach
Taq-DNA-Polymerase	NEB	Schwalbach
TCEP	Pierce	ckford, USA
Tev Proteas	Invitrogen	San Diego, USA
TEMED	Roth	Karlsruhe
Tricin ultra pure	ICN	Eschwege
Tris ultra pure	ICN	Eschwege
Triton X-100	Sigma	Deisenhofen
Trypsin, modified, sequencing grade	Promega	Mannheim
Tween 20	Sigma	Deisenhofen

5.1.4 Kits

Chemical:	Specification/Manufacturer	City
Expand LongTemplate PCR System	Roche	Mannheim
QIAprep Spin Miniprep-Kit	Qiagen	Hilden
QIAquick Gel Extraktion-Kit	Qiagen	Hilden
QuikChange XL Site-Directed mutagenesis kit	Stratagene	La Jolla/USA
Western Lightning Western-Blot Detection Kit	Pierce	Ckford, USA

5.2 Methods

5.2.1 Cells and cell culture

Sf9 cells are derived from IPLB-Sf21-AE, an established cell line originally isolated from *Spodoptera frugiperda* ovaries. This cell line was maintained as a suspension culture in a glass flask by continuous rotation (135 rpm) at 26°C and maintained at a densities of 0.6 –3.0 x 10^6 cells / ml in complete IPL-41 medium (JRH Biosciences, Lenexa, KS, USA), which supplemented with Pluronic F68 (10%)

5.2.2 Construction of the expression plasmids pSEAP-haCerse

To generate the recombinant baculovirus expressing the human acid ceramidase precursor, a fusion construct of secretory alkaline phosphatase (SEAP)-Tev cleavage site-acid ceramidase (haCerase) -Tev cleavage site-6His-tag was designed. The full-length cDNAs encoding acid ceramidase or SEAP were used as the templates to generate the new expression plasmids. For this purpose, the different genetic building blocks were amplified in several PCRs using “Expand LongTemplate PCR System” (Roche). For the amplification of SEAP-Tev cleavage site open reading frame from pSEAP2-Basic (clontech), forward primer (Sigma-Genosys) 5_ GATCAGATCTTCGCGAATTCGCCCACCATGCTGCTGCTGCTGCTGCTG-3 _ (with the added Bgl II site underlined) and reverse primer 5_-CATCGTCGAC**GCCCTGAAAATACAGGTTTTC**TGTCTGCTCGAAGCGG CCGGC-3_ (with the added Sal I site underlined and Tev protease cleavage site in bold). In order to construct haCerase with an additional

carboxyl-terminal sequence 6x histidine affinity tag and Tev protease cleavage site, we prepared a cDNA fragment by PCR with forward primer 5_-GATCGTCGACCAGCACGCGCCGCCGTGGACAGAGGACTGCAGAAAA TCAACC-3_ (with added Sal I site underlined) and reverse primer 5_-CATCGGTACC*GTGATGGTGATGGTGATG*GGTCGTTGGGATATCGTAA TC**GCCCTGAAAATACAGGTTTTC**CCAACCTATACAAGGGTCAGG-3_ (with the added Kpn I site underlined, 6x histidine in italic and Tev protease cleavage site in bold) were used to amplify the haCerase open reading from pCR-XL Topo vector (Leber, 1999) .

Prepare the sample PCR reaction(s) as indicated below:

5 μl of 10× reaction buffer
1.5 μl (10 ng) of dsDNA template
1 μl (20 pmol) of oligonucleotide downstream primer
1 μl (20 pmol) of oligonucleotide upstream primer
2.5 μl of dNTP (10 mM) mix
ddH2O to a final volume of 50 μl
Then add 0.75 μl of DNA polymerase (5 U/μl)

Following PCR program:

1 x cycle: 94 °C, 3 min. (Initial denaturation)
15 x cycle: a) 94 °C, 15 sec. (Denaturation)
b) 55 °C, 1 min. (Annealing)
c) 68 °C, 2 min. (Elongation)
1 x cycle: 68 °C, 5 min. (Final elongation)

The PCR products: “SEAP-Tev” and “haCerase-6x His-Tev” fragments were digested by Bgl II, Sal I and Kpn I restriction enzymes then ligated into between the BamH I site and Kpn I site of the pFastBac transfer vector

(Invitrogen). The resulting plasmids were termed pSEAP-haCerase with a size of ~ 7584 bp. The recombinant plasmid was propagated in *Escherichia coli* DH5α.

5.2.3 Construction of the expression plasmids pSEAP-haCerse*mut*

The QuikChange XL Site-Directed mutagenesis kit (Stratagene) was used to generate the pSEAP-haCerase*mut* vector expressing individually seven different point mutants (Thr141Val, Ile142Val, Cys143Ala, Cys143Met, Thr144Ala, Ser145Ala and Ser145Thr) of haCerase were conducted in accordance to manufacturer's recommendations. Only the PCR program was changed. (Cys143 of haCerase is the N-terminal amino acid of the β-subunit and is assumed to be the nucleophile of the catalytic center.) Seven pairs of complementary oligonucleotides (Sigma-Genosys) were used (The mutated codon are indicated in bold).

T141V: upstream primer:
5_-CAATATTTTTTATGAATTATTT**GTC**ATTTGTACTTCAATAGTAGCAGAAG-3_.
downstream primer:
5_-CTTCTGCTACTATTGAAGTACAAAT**GAC**AAATAATTCATAAAAAATATTG-3_.
I142V: upstream primer:
5_- GAATTATTTACC**GTT**TGTACTTCAATAGTAGCAGAAGACAAAAAAGGTC-3_.
downstream primer:
5_- GACCTTTTTTGTCTTCTGCTACTATTGAAGTACA**AAC**GGTAAATAATTC-3_.
C143A: upstream primer:
5_- GAATTATTTACCATT**GCT**ACTTCAATAGTAGCAGAAGACAAAAAAGGTC-3_.
downstream primer:
5_-GACCTTTTTTGTCTTCTGCTACTATTGAAGT**AGC**AATGGTAAATAATTC-3_.
C143M: upstream primer:
5_- GAATTATTTACCATT**ATG**ACTTCAATAGTAGCAGAAGACAAAAAAGGTC-3_.
downstream primer:

5_- GACCTTTTTTGTCTTCTGCTACTATTGAAGT**CAT**AATGGTAAATAATTC-3_.
T144A: upstream primer:
5_- GAATTATTTACCATTTGT**GCT**TCAATAGTAGCAGAAGACAAAAAAGGTC-3_.
downstream primer:
5_- GACCTTTTTTGTCTTCTGCTACTATTGA**AGC**ACAAATGGTAAATAATTC-3_.
S145A: upstream primer:
5_- GAATTATTTACCATTTGTACT**GCT**ATAGTAGCAGAAGACAAAAAAGGTC-3_.
downstream primer:
5_- GACCTTTTTTGTCTTCTGCTACTAT**AGC**AGTACAAATGGTAAATAATTC-3_.
S145T: upstream primer:
5_- GAATTATTTACCATTTGTACT**ACT**ATAGTAGCAGAAGACAAAAAAGGTC-3_.
downstream primer:
5_- GACCTTTTTTGTCTTCTGCTACTAT**AGT**AGTACAAATGGTAAATAATTC-3_.

Prepare the sample PCR reaction(s) as indicated below:

5 µl of 10× reaction buffer
1 µl (30 ng) of dsDNA template: pSEAP-haCerase
1 µl (125 ng) of oligonucleotide downstream primer
1 µl (125 ng) of oligonucleotide upstream primer
2 µl of dNTP mix
3 µl of QuickSolution
ddH2O to a final volume of 50 µl
Then add 1 µl *PfuTurbo* DNA polymerase (2.5 U/ µl)

Following PCR program:

1 x cycle: 95 °C, 1 min. (Initial denaturation)
16 x cycle: a) 95 °C, 50 sec. (Denaturation)
b) 64 °C, 50 sec. (Annealing)
c) 68 °C, 10 min. (Elongation)
1 x cycle: 68 °C, 7 min. (Final elongation)

After transformation into XL10-Gold ultracompetent cells, the mutant sites were sequenced again (SeqLab GmbH).

5.2.4 Recombinant fusion protein expression

For expression in Sf9 insect cells according to Bac-to-Bac baculovirus expression system protocol, the recombinant plasmids (pSEAP-haCerase or pSEAP-haCerase*mut*) constructs were transformed into *E. coli* DH10Bac-competent cells containing the circular baculovirus genone to generate recombinant bacmids per manufacturer's protocol (Invitrogen). The Bacmid DNAs were prepared and transfected into Sf9 cells using Transfection Buffer A and B Set (BD Biosciences) to produce recombinant baculoviruses that were amplified with a titler of 3.2 x 10^8 PFU/ml and used to express wild type: "SEAP-haCease" fusion protein or mutant: "SEAP-haCerase*mu"t* fusion protein in insect cells.

5.2.5 Purification of recombinant acid ceramidase

For preparative expression and purification of mutant fusion protein (Cys143Ala), stably transformed Sf9 cells were cultured as 800 mL suspension cultures in 2 L flask to a final density of 2.2 x 10^6 cells/mL. Since the expression level reached an approximate plateau after 96 hours, at this time point, the medium was harvested by centrifugation (6500 rpm, 30 min.) and kept at 4°C. The supernatant was then concentrated 10-fold by VivaFlow 200 (Vivascience) with filter-membrane 100,000 MW (PES), and then the concentrated medium exchanged to DEAE-Sepharose equilibration buffer (50 mM Tris/HCl; 100 mM NaCl, pH 7.4) by dialysis (Serva) overnight. After centrifugation (10000 rpm, 30 min.), the buffer-exchanged supernatant (200 ml) was then loaded with a rate of 2 ml/min onto DEAE-Sepharose (column dimensions: 2.6 x 15 cm, Sigma), which was pre-equilibrated with

wash buffer (50 mM Tris-HCl, 100 mM NaCl, pH 7.4). The suspension of flow-through was collected. After overnight dialysis with Ni-NTA wash buffer (50 mM NaH_2PO_4, 300 mM NaCl, 20 mM imidazole, pH 7.8), the suspension was clarified by centrifugation (10000 rpm, 30 min) and sterile filtration (0.2 μm). The filtrate was loaded with a rate of 1 ml/min onto a Ni-NTA superflow column (column dimensions: 1.6 x 4.5 cm, Qiagen). After the column was washed with 4 column volumes of Ni-NTA wash buffer, absorbed proteins were direct eluted in 20 ml elution buffer (50 mM NaH_2PO_4, 300 mM NaCl, 125 mM imidazole (pH 7.8)). The eluted sample was then concentrated 5-fold by Vivaspin 20 concentrater (Vivascience) with filter-membrane 100,000 MW (PES), 2000 rpm, and then the concentrated sample (final volume:~2 ml) was loaded with a rate of 1 ml/min onto gel filtration column: Superdex 75 Hiload 16/60 with running buffer (50 mM Tris/HCl, 200 mM NaCl, pH 7.6) in FPLC system (GE Healthcare). Pooled fusion protein “SEAP-haCerasemut” fractions (Number:14~19.) were concentrated (final volume: ~2 ml) and buffer exchange with Tev-buffer (50 mM Tris/HCl, pH 7.6, 0.5 mM EDTA, 1 mM DTT) using Vivaspin 20 (Vivascience). AcTEV protease (Invitrogen) cleavage reaction was performed for three hours at room temperature following manufacturer’s protocol. The digested sample was loaded again onto the same gel fitration column: Superdex 75 Hiload 16/60 in FPLC system. The new appeared peak´s fractions were collected, containing the purified enzyme ”haCerase” without SEAP and 6x histidine amino acids.

5.2.6 Determination of acid ceramidase activity with a micellar assay system

Acid ceramidase activity in the detergent-containing micellar assay system was measured, with minor Modification, according to Bernardo *et al.* (1995).

5.2.6.1 Composition of incubation mixture and assay conditions

The incubation mixture contained in a final volume of 100 µl: 10-50 µl undiluted enzyme solution, 17 nmol N-lauroyl sphingosine, solubilized in 0.5 % (w/v) Triton X-100, 0.2 % (w/v) Tween 20, 0.2 % (w/v) NP-40 and 0.8 % (w/v) sodium cholate, 250 mM sodium acetate buffer (pH 4.0) and 5 mM EDTA. The enzyme assays were incubated for 30 min at 37 °C.

5.2.6.2 Sample preparation and HPLC analysis of sphingoid bases

Enzyme reaction was terminated by adding 800 µl HPLC-grade (2:1, v/v) chloroform/methanol and 200 µl of 100 mM ammonium hydrogen carbonate solution. D-erythro-1,3-dihydroxy-2-aminotetradecane (C_{14}-sphinganine) and D-erythro-1,3-dihydroxy-2-aminohexadecane (C_{16}--sphinganine), solubilized in HPLC-grade methanol, were added to the incubation mixture as internal standards (500 pmol each). Samples were mixed for 10 min and then centrifuged for 5 min at 10,000 x g. The lower chloroform phase containing the liberated sphingosine and internal standards was carefully removed and collected in a fresh vial. For quantitative recovery of sphingosine and the internal standards the extraction was repeated by adding 600 µl (2:1 v/v) chloroform/methanol to each incubation vial. The following extraction steps were performed as described above. The combined organic phases were evaporated to dryness under a stream of nitrogen. The dried enzyme assays

were solubilized in 50 µl HPLC-grade ethanol and mixed for 10 min at 50°C. Samples had cooled down to room temperature. 50 µl Fluoroaldehyde (Pierce) were added to each incubation vial. Alternatively, o-phtaldialdehyde reagent solution was prepared as follows: 100 µl of an ethanol solution containing 5 mg of o-phtalaldehyde and 5 µl β-mercaptoethanol were added to 9.9 ml of a 3 % (w/v) boric acid solution, adjusted to pH 10.5 with KOH. Samples were mixed for 5 min at room temperature and then diluted with 0.9 ml HPLC buffer (acetonitril/2 mM potassium phosphate, pH 7.0, 9/1 v/v) to a final volume of 1 ml. An aliquot of each sample (100-200 µl) was injected onto a LiChroCART 125-4 Nucleosil 5 C18-column (125 x 4 mm, Merck), equilibrated in HPLC buffer. The derivatized sphinganine and sphingosine bases were eluted isocratically (flow rate: 1 ml/min, Shimadzu LC-10 AT solvent delivery system) and detected by a fluorescence detector (Shimadzu RF-10 AX, excitation wavelength: 355 nm, emission wavelength: 435 nm). Quantification of liberated sphingosine was performed with a Window based standard liquid Chromatography software (Class CR-10, Shimadzu).

5.2.7 Protein quantification

Protein concentrations were determined with the BCA method (Smith et al. 1985). Concentration measurements were carried out in duplicates in a 96-well microtiter plate. Protein containing samples (20 µl) were mixed with 200 µl of a BCA-copper sulfate solution. The BCA-copper sulfate solution was prepared by mixing 49 parts of BCA solution (pH 11.5) with 1 part 4 % (w/v) copper sulfate solution. Samples were incubated for 30 min at 60°C. Under the alkaline assay conditions proteins reduce Cu (II) to Cu (I) which forms a

complex with BCA. The Cu (l) -BCA complex was measured at 595 nm in a microplate photometer. Protein concentrations were determined by comparison to a calibration curve generated with BSA solution of known concentration (0-5 μg/20 μl).

5.2.8 SDS-PAGE analysis

SDS-PAGE analysis of proteins was performed according to the protocol of Schägger and von Jagow (Schagger et al. 1987). Proteins were heated in sample buffer (3.0 M Tris/HCl, pH 8.45; 0.3 % SDS; ± 5 % (v/v) β-mercaptoethanol) for 5 min at 95°C. Denatured proteins were electrophoresed in a mini-gel apparatus (100 x 70 x 0.75 mm, Biorad) with 4 % concentration gel (running distance 1 cm) and 8 % separation gel (running distance 6 cm). Electrophoresis was first carried out at 20 mA constant current until the dye front reached the separation gel. The current was then raised to constant 30 mA. Electrophoresis was terminated when the dye front reached the bottom of the gel.

5.2.9 Visualization of proteins by colloidal Coomassie Blue R 250

After electrophoresis, gels were incubated for 60 min in a fixation solution (40 % MeOH, 10 % AcOH (v/v)). Gels were stained for 2 hours with a colloidal Coomassie Blue solution (ICN). Image enhancement was achieved by incubating the gel for 10 min with a developer solution (25 % EtOH, 8 % AcOH (v/v)). Gels were destained with an acetic acid solution (10 % (v/v)).

5.2.10 Silver staining of proteins

Silver staining of proteins in SDS-PAGE gels was carried out according to . After electrophoresis, gels were incubated for 60 min in a fixation solution (50 % (v/v) MeOH, 12 % (v/v) AcOH, 0.5 ml/L formaldehyde solution 37 % (v/v)). Gels were then washed 3 x 20 min with 50 % (v/v) EtOH. After the washing step, gels were treated for 1 min with incubation solution (0.2 g/L $Na_2S_2O_3$ x 5 H_2O). Gels were then impregnated for 20 min with a silver ion solution (2 g/L $AgNO_3$, 0.75ml/L formaldehyde solution (37 %)). Excess silver stain was removed by washing the gels briefly with water. Proteins were visualized by incubating the gel with developing solution (60 g/L Na_2CO_3, 4 mg/L $Na_2S_2O_3$ x 5 H_2O, 0.5 ml/L formaldehyde solution (37 %)). Development was terminated with a stop solution (50 % (v/v) MeOH, 12 % (v/v) AcOH) as soon as the first protein bands became visible. In order to remove excess acetic acid a final fixation step (30 % (v/v) MeOH, 3 % glycerol) was carried out. Gels were air dried between two cellulose sheets.

5.2.11 Western blot analysis

Immunochemical detection of SDS-PAGE separated proteins was carried out after proteins were electrophoretically transfered onto PVDF membranes using a tank blotting procedure. After electrophoresis, gels were equilibrated for 15 min in transfer buffer (10 mM 3-(cyclohexylamino)- 1-propanesulfonic acid (CAPS) buffer, pH 11, 10% (v/v) methanol). After equilibration, gels were laid on top of a MeOH-wetted PVDF membrane. Protein transfer was performed at a current of 400 mA for 36 min in a Mini-Trans-Blot apparatus (Biorad). After transfer of proteins, PVDF membranes were incubated for 60 min at room

temperature with blocking solution (5% low-fat milk in TBST buffer (10 mM Tris-HCl pH 8, 150 mM NaCl and 0.05% Tween 20) and than incubated with polyclonal rabbit anti-human acid ceramidase antiserum (dilution 1:1000) raised against expressed human acid ceramidase. The membrane was washed three times with TBST buffer. Detection of acid ceramidase was performed using antirabbit- IgG-HRP conjugate as secondary antibody (diluted 1:10,000 in TBST). Proteins were visualized with the SuperSignal west pico chemiluminescent substrate Kit (Pierce).

5.2.12 In-gel tryptic digestion and MALDI Mass spectrometry

The purified recombinant fusion proteins (0.8 mg) were running onto the lane of 8% SDS PAGE under reducing condition. After Coomassie-staining, the bands of recombinant fusion protein “SEAP-haCerase” were excised as gel slices and then were incubated with modified trypsin (Promega) overnight at 37°C. The tryptic peptides were extracted according to standard protocol (Shevchenko et al. 2006) prior to Mass spectrometry.

MALDI-TOF-MS analysis was performed in positive mode on a TofSpec E mass spectrometer (Micromass) with a 337 nm nitrogen laser. The acceleration voltage was set to 20 kV. An extraction voltage of 19.5 kV and a focus voltage of 15.5 kV were used. A pulse voltage of 2200–2400 V was used for measurements in the reflectron mode and of 1200 V for measurements in the linear mode with the high mass detector. Measurements were performed at threshold laser energy. α-Cyano-4-hydroxycinnamic acid (Sigma) (10 mg/ml in 50% acetonitrile (Merck), 50% water containing 0.1% trifluoroacetic acid (Sigma)) for peptides or sinapinic acid (Sigma) (10 mg/ml in 40% acetonitrile,

60% water containing 0.1% trifluoroacetic acid) for proteins were used as matrices. The peptide solution was mixed with the matrix solution (each 1 μl) on the target and dried at room temperature. Calibration was performed using standard peptides.

5.2.13 Cross-linking experiment between acid ceramidase and Sap D

5.2.13.1 Cross-linking test *in vivo*

Labeling with L-photo-Leucine:

BHK (baby hamster kidney) cells were grown in high-glucose DMEM (Gibco; with L-glutamine and sodium pyruvate) with 10% fetal calf serum (FCS). Typically, 5 cm^2 of cells are needed for a cross-linking experiment with detection by Western blot. At about 70% confluence, medium was replaced by DMEM-LM (DMEM lacking L-leucine and L-Methionine, supplemented with 5% dialyzed FCS and 30 mg/L L-Methionine). L-photo-Leucine was added to a final concentration of 4 mM, and cells were cultivated for 24 h, washed with phosphate-buffered saline (PBS) and UV-irradiated using a 365 nm lamp for 15 min. The samples were placed at a distance of 4 cm from the light source. Cells were harvested, washed twice with PBS, and resuspended in lysis (RIPA) buffer (10 mM Tris pH 7.5, 150 mM NaCl, 10% glycerol, 1% NP-40, 5 mM EDTA) containing a cocktail of protease inhibitors (Roche Diagnostics). Cell lysates were centrifuged for 15 min at 14 000 rpm. Supernatants were collected following by SDS PAGE and Western blot as above.

Chemical cross-linking:

BHK cells were grown in DMEM, washed with PBS, incubated with 1% paraformaldehyde (PFA) in PBS for 30 min on ice, and finally quenched for 15

min with10 mM Tris (pH 8.5). Cell lysis and processing for SDS PAGE and Western blot was done as above.

5.2.13.2 Cross-linking test *in vitro*

Due to the presence of amino group in Tris/HCl buffer, the Tris/HCl buffer of gel filtration in FPLC system was exchanged with PBS buffer (100 mM phosphate, 200 mM NaCl, pH 7.6). After Tev cleavage reaction, the sample was loaded into FPLC with PBS buffer and then the purified acid ceramidase was ready for cross-linking test.

Add a 48-fold molar excess of DSG (between 0.25-5 mM) to the protein sample (acid ceramidase and Sap-D in molar ratio 1:1 or 1:2) at room temperature for 30 min, and finally quenched for 15 min with 500 mM Tris (pH 8.5). The treated sample for SDS PAGE and Western blot was done as above.

6 References

Alanko SM, Halling KK, Maunula S, Slotte JP, Ramstedt B (2005) Displacement of sterols from sterol/sphingomyelin domains in fluid bilayer membranes by competing molecules. Biochim Biophys Acta 1715: 111-21

Altschul SF, Madden TL, Schaffer AA, Zhang J, Zhang Z, Miller W, Lipman DJ (1997) Gapped BLAST and PSI-BLAST: a new generation of protein database search programs. Nucleic Acids Res 25: 3389-402

Bär J, Linke T, Ferlinz K, Neumann U, Schuchman EH, Sandhoff K (2001) Molecular analysis of acid ceramidase deficiency in patients with Farber disease. Hum Mutat 17: 199-209

Becker KP, Kitatani K, Idkowiak-Baldys J, Bielawski J, Hannun YA (2005) Selective inhibition of juxtanuclear translocation of protein kinase C betaII by a negative feedback mechanism involving ceramide formed from the salvage pathway. J Biol Chem 280: 2606-12

Bernardo K, Hurwitz R, Zenk T, Desnick RJ, Ferlinz K, Schuchman EH, Sandhoff K (1995) Purification, characterization, and biosynthesis of human acid ceramidase. J Biol Chem 270: 11098-102

Bieberich E (2008) Ceramide signaling in cancer and stem cells. Future Lipidol 3: 273-300

Bochtler M, Ditzel L, Groll M, Hartmann C, Huber R (1999) The proteasome. Annu Rev Biophys Biomol Struct 28: 295-317

Bollinger CR, Teichgraber V, Gulbins E (2005) Ceramide-enriched membrane domains. Biochim Biophys Acta 1746: 284-94

Carrington JC, Dougherty WG (1988) A viral cleavage site cassette: identification of amino acid sequences required for tobacco etch virus polyprotein processing. Proc Natl Acad Sci USA 85: 3391-5

Chandra PM, Brannigan JA, Prabhune A, Pundle A, Turkenburg JP, Dodson GG, Suresh CG (2005) Cloning, preparation and preliminary crystallographic studies of penicillin V acylase autoproteolytic processing mutants. Acta Crystallogr Sect F Struct Biol Cryst Commun 61: 124-7

Chiantia S, Kahya N, Schwille P (2007) Raft domain reorganization driven by short- and long-chain ceramide: a combined AFM and FCS study. Langmuir 23: 7659-65

Chiantia S, Ries J, Chwastek G, Carrer D, Li Z, Bittman R, Schwille P (2008) Role of ceramide in membrane protein organization investigated by combined AFM and FCS. Biochim Biophys Acta 1778: 1356-64

Ciaffoni F, Salvioli R, Tatti M, Arancia G, Crateri P, Vaccaro AM (2001) Saposin D solubilizes anionic phospholipid-containing membranes. J Biol Chem 276: 31583-9

Cuvillier O (2002) Sphingosine in apoptosis signaling. Biochim Biophys Acta 1585: 153-62

Cuvillier O, Edsall L, Spiegel S (2000) Involvement of sphingosine in mitochondria-dependent Fas-induced apoptosis of type II Jurkat T cells. J Biol Chem 275: 15691-700

Cuvillier O, Nava VE, Murthy SK, Edsall LC, Levade T, Milstien S, Spiegel S (2001) Sphingosine generation, cytochrome c release, and activation of

caspase-7 in doxorubicin-induced apoptosis of MCF7 breast adenocarcinoma cells. Cell Death Differ 8: 162-71

Cuvillier O, Pirianov G, Kleuser B, Vanek PG, Coso OA, Gutkind S, Spiegel S (1996) Suppression of ceramide-mediated programmed cell death by sphingosine-1-phosphate. Nature 381: 800-3

Edinger AL (2009) Starvation in the midst of plenty: making sense of ceramide-induced autophagy by analysing nutrient transporter expression. Biochem Soc Trans 37: 253-8

Eggeling C, Ringemann C, Medda R, Schwarzmann G, Sandhoff K, Polyakova S, Belov VN, Hein B, von Middendorff C, Schonle A, Hell SW (2008) Direct observation of the nanoscale dynamics of membrane lipids in a living cell. Nature

El Bawab S, Roddy P, Qian T, Bielawska A, Lemasters JJ, Hannun YA (2000) Molecular cloning and characterization of a human mitochondrial ceramidase. J Biol Chem 275: 21508-13

Farber S (1952) A lipid metabolic disorder: disseminated lipogranulomatosis; a syndrome with similarity to, and important difference from, Niemann-Pick and Hand-Schuller-Christian disease. AMA Am J Dis Child 84: 499-500

Ferlinz K, Kopal G, Bernardo K, Linke T, Bar J, Breiden B, Neumann U, Lang F, Schuchman EH, Sandhoff K (2001) Human acid ceramidase: processing, glycosylation, and lysosomal targeting. J Biol Chem 276: 35352-60

Fukasawa M, Nishijima M, Hanada K (1999) Genetic evidence for ATP-dependent endoplasmic reticulum-to-Golgi apparatus trafficking of

ceramide for sphingomyelin synthesis in Chinese hamster ovary cells. J Cell Biol 144: 673-85

Furst W, Sandhoff K (1992) Activator proteins and topology of lysosomal sphingolipid catabolism. Biochim Biophys Acta 1126: 1-16

Gallala H, Sandhoff K (2008) Principles of microdomain formation in biological membranes—Are there lipid liquid ordered domains in living cellular membranes? Trends in Glycosci Glycotechnol 20: 277–295

Gillard BK, Clement R, Colucci-Guyon E, Babinet C, Schwarzmann G, Taki T, Kasama T, Marcus DM (1998a) Decreased synthesis of glycosphingolipids in cells lacking vimentin intermediate filaments. Exp Cell Res 242: 561-72

Gillard BK, Clement RG, Marcus DM (1998b) Variations among cell lines in the synthesis of sphingolipids in de novo and recycling pathways. Glycobiology 8: 885-90

Gillard BK, Harrell RG, Marcus DM (1996) Pathways of glycosphingolipid biosynthesis in SW13 cells in the presence and absence of vimentin intermediate filaments. Glycobiology 6: 33-42

Gonzalez C, Langdon GM, Bruix M, Galvez A, Valdivia E, Maqueda M, Rico M (2000) Bacteriocin AS-48, a microbial cyclic polypeptide structurally and functionally related to mammalian NK-lysin. Proc Natl Acad Sci U S A 97: 11221-6

Grassme H, Jekle A, Riehle A, Schwarz H, Berger J, Sandhoff K, Kolesnick R, Gulbins E (2001) CD95 signaling via ceramide-rich membrane rafts. J Biol Chem 276: 20589-96

Grassme H, Jendrossek V, Riehle A, von Kurthy G, Berger J, Schwarz H, Weller M, Kolesnick R, Gulbins E (2003) Host defense against Pseudomonas aeruginosa requires ceramide-rich membrane rafts. Nat Med 9: 322-30

Guenther GG, Peralta ER, Rosales KR, Wong SY, Siskind LJ, Edinger AL (2008) Ceramide starves cells to death by downregulating nutrient transporter proteins. Proc Natl Acad Sci U S A 105: 17402-7

Hanada K, Kumagai K, Yasuda S, Miura Y, Kawano M, Fukasawa M, Nishijima M (2003) Molecular machinery for non-vesicular trafficking of ceramide. Nature 426: 803-9

Hannun YA, Luberto C, Argraves KM (2001) Enzymes of sphingolipid metabolism: from modular to integrative signaling. Biochemistry 40: 4893-903

Hannun YA, Obeid LM (2008) Principles of bioactive lipid signalling: lessons from sphingolipids. Nat Rev Mol Cell Biol 9: 139-50

Heung LJ, Kaiser AE, Luberto C, Del Poeta M (2005) The role and mechanism of diacylglycerol-protein kinase C1 signaling in melanogenesis by Cryptococcus neoformans. J Biol Chem 280: 28547-55

Jones BV, Begley M, Hill C, Gahan CG, Marchesi JR (2008) Functional and comparative metagenomic analysis of bile salt hydrolase activity in the human gut microbiome. Proc Natl Acad Sci U S A 105: 13580-5

Karlsson KA (1989) Animal glycosphingolipids as membrane attachment sites for bacteria. Annu Rev Biochem 58: 309-50

Kitatani K, Idkowiak-Baldys J, Bielawski J, Taha TA, Jenkins RW, Senkal CE, Ogretmen B, Obeid LM, Hannun YA (2006) Protein kinase C-induced

activation of a ceramide/protein phosphatase 1 pathway leading to dephosphorylation of p38 MAPK. J Biol Chem 281: 36793-802

Kitatani K, Idkowiak-Baldys J, Hannun YA (2008) The sphingolipid salvage pathway in ceramide metabolism and signaling. Cell Signal 20: 1010-8

Klein A, Henseler M, Klein C, Suzuki K, Harzer K, Sandhoff K (1994) Sphingolipid activator protein D (sap-D) stimulates the lysosomal degradation of ceramide in vivo. Biochem Biophys Res Commun 200: 1440-8

Ko YG, Liu P, Pathak RK, Craig LC, Anderson RG (1998) Early effects of pp60(v-src) kinase activation on caveolae. J Cell Biochem 71: 524-35

Koch J, Gartner S, Li CM, Quintern LE, Bernardo K, Levran O, Schnabel D, Desnick RJ, Schuchman EH, Sandhoff K (1996) Molecular cloning and characterization of a full-length complementary DNA encoding human acid ceramidase. Identification Of the first molecular lesion causing Farber disease. J Biol Chem 271: 33110-5.

Kolter T, Sandhoff K (2005) Principles of lysosomal membrane digestion: stimulation of sphingolipid degradation by sphingolipid activator proteins and anionic lysosomal lipids. Annu Rev Cell Dev Biol 21: 81-103

Kolter T, Winau F, Schaible UE, Leippe M, Sandhoff K (2005) Lipid-binding proteins in membrane digestion, antigen presentation, and antimicrobial defense. J Biol Chem 280: 41125-8

Kumar RS, Brannigan JA, Prabhune AA, Pundle AV, Dodson GG, Dodson EJ, Suresh CG (2006) Structural and functional analysis of a conjugated bile salt hydrolase from Bifidobacterium longum reveals an evolutionary relationship with penicillin V acylase. J Biol Chem 281: 32516-25

Li CM, Hong SB, Kopal G, He X, Linke T, Hou WS, Koch J, Gatt S, Sandhoff K, Schuchman EH (1998) Cloning and characterization of the full-length cDNA and genomic sequences encoding murine acid ceramidase. Genomics 50: 267-74.

Li CM, Park JH, He X, Levy B, Chen F, Arai K, Adler DA, Disteche CM, Koch J, Sandhoff K, Schuchman EH (1999) The human acid ceramidase gene (ASAH): structure, chromosomal location, mutation analysis, and expression. Genomics 62: 223-31.

Linke T (2000) Purification, enzymatic characterization and interfacial activity of human acid ceramidase. PhD, University of Bonn

Linke T, Lansmann S, Sandhoff K (2000) Purification of acid ceramidase from human placenta. Methods Enzymol 311: 201-7

Linke T, Wilkening G, Sadeghlar F, Mozcall H, Bernardo K, Schuchman E, Sandhoff K (2001) Interfacial regulation of acid ceramidase activity. Stimulation of ceramide degradation by lysosomal lipids and sphingolipid activator proteins. J Biol Chem 276: 5760-8

Liu H, Sugiura M, Nava VE, Edsall LC, Kono K, Poulton S, Milstien S, Kohama T, Spiegel S (2000) Molecular cloning and functional characterization of a novel mammalian sphingosine kinase type 2 isoform. J Biol Chem 275: 19513-20

Luckow VA, Lee SC, Barry GF, Olins PO (1993) Efficient generation of infectious recombinant baculoviruses by site-specific transposon-mediated insertion of foreign genes into a baculovirus genome propagated in Escherichia coli. J Virol 67: 4566-79

Mandon EC, Ehses I, Rother J, van Echten G, Sandhoff K (1992) Subcellular localization and membrane topology of serine palmitoyltransferase, 3-dehydrosphinganine reductase, and sphinganine N-acyltransferase in mouse liver. J Biol Chem 267: 11144-8

Mao C, Xu R, Szulc ZM, Bielawska A, Galadari SH, Obeid LM (2001) Cloning and characterization of a novel human alkaline ceramidase. A mammalian enzyme that hydrolyzes phytoceramide. J Biol Chem 276: 26577-88

Mao C, Xu R, Szulc ZM, Bielawski J, Becker KP, Bielawska A, Galadari SH, Hu W, Obeid LM (2003) Cloning and characterization of a mouse endoplasmic reticulum alkaline ceramidase: an enzyme that preferentially regulates metabolism of very long chain ceramides. J Biol Chem 278: 31184-91

Mathias S, Pena LA, Kolesnick RN (1998) Signal transduction of stress via ceramide. Biochem J 335 (Pt 3): 465-80

Megha, London E (2004) Ceramide selectively displaces cholesterol from ordered lipid domains (rafts): implications for lipid raft structure and function. J Biol Chem 279: 9997-10004

Megha, Sawatzki P, Kolter T, Bittman R, London E (2007) Effect of ceramide N-acyl chain and polar headgroup structure on the properties of ordered lipid domains (lipid rafts). Biochim Biophys Acta 1768: 2205-12

Mitsutake S, Tani M, Okino N, Mori K, Ichinose S, Omori A, Iida H, Nakamura T, Ito M (2001) Purification, characterization, molecular cloning, and subcellular distribution of neutral ceramidase of rat kidney. J Biol Chem 276: 26249-59

Möbius W, van Donselaar E, Ohno-Iwashita Y, Shimada Y, Heijnen HF, Slot JW, Geuze HJ (2003) Recycling compartments and the internal vesicles of multivesicular bodies harbor most of the cholesterol found in the endocytic pathway. Traffic 4: 222-31

Mocchetti I (2005) Exogenous gangliosides, neuronal plasticity and repair, and the neurotrophins. Cell Mol Life Sci 62: 2283-94

Munro S (2003) Lipid rafts: elusive or illusive? Cell 115: 377-88

Ogretmen B, Pettus BJ, Rossi MJ, Wood R, Usta J, Szulc Z, Bielawska A, Obeid LM, Hannun YA (2002) Biochemical mechanisms of the generation of endogenous long chain ceramide in response to exogenous short chain ceramide in the A549 human lung adenocarcinoma cell line. Role for endogenous ceramide in mediating the action of exogenous ceramide. J Biol Chem 277: 12960-9

Oinonen C, Rouvinen J (2000) Structural comparison of Ntn-hydrolases. Protein Sci 9: 2329-37

Okazaki T, Bielawska A, Bell RM, Hannun YA (1990) Role of ceramide as a lipid mediator of 1 alpha,25-dihydroxyvitamin D3-induced HL-60 cell differentiation. J Biol Chem 265: 15823-31

Olivera A, Spiegel S (1993) Sphingosine-1-phosphate as second messenger in cell proliferation induced by PDGF and FCS mitogens. Nature 365: 557-60

Remmel N, Locatelli-Hoops S, Breiden B, Schwarzmann G, Sandhoff K (2007) Saposin B mobilizes lipids from cholesterol-poor and bis(monoacylglycero)phosphate-rich membranes at acidic pH.

Unglycosylated patient variant saposin B lacks lipid-extraction capacity. Febs J 274: 3405-20

Rossmann M, Schultz-Heienbrok R, Behlke J, Remmel N, Alings C, Sandhoff K, Saenger W, Maier T (2008) Crystal structures of human saposins C andD: implications for lipid recognition and membrane interactions. Structure 16: 809-17

Rossocha M, Schultz-Heienbrok R, von Moeller H, Coleman JP, Saenger W (2005) Conjugated bile acid hydrolase is a tetrameric N-terminal thiol hydrolase with specific recognition of its cholyl but not of its tauryl product. Biochemistry 44: 5739-48

Sandhoff K, Kolter T (2003) Biosynthesis and degradation of mammalian glycosphingolipids. Philos Trans R Soc Lond B Biol Sci 358: 847-61

Sandhoff K, Kolter T, Harzer K (2001) Sphingolipid Activator Proteins. The Metabolic and Molecular Bases of Inherited Disease, 8th edn, vol Vol. III, pp 3371 – 3389

Schagger H, Borchart U, Machleidt W, Link TA, Von Jagow G (1987) Isolation and amino acid sequence of the 'Rieske' iron sulfur protein of beef heart ubiquinol:cytochrome c reductase. FEBS Lett 219: 161-8

Schulze H, Schepers U, Sandhoff K (2007) Overexpression and mass spectrometry analysis of mature human acid ceramidase. Biol Chem 388: 1333-43

Schwarzmann G, Sandhoff K (1990) Metabolism and intracellular transport of glycosphingolipids. Biochemistry 29: 10865-71

Seemuller E, Lupas A, Baumeister W (1996) Autocatalytic processing of the 20S proteasome. Nature 382: 468-71

Shah J, Atienza JM, Rawlings AV, Shipley GG (1995) Physical properties of ceramides: effect of fatty acid hydroxylation. J Lipid Res 36: 1945-55

Shevchenko A, Tomas H, Havlis J, Olsen JV, Mann M (2006) In-gel digestion for mass spectrometric characterization of proteins and proteomes. Nat Protoc 1: 2856-60

Shtraizent N, Eliyahu E, Park JH, He X, Shalgi R, Schuchman EH (2008) Autoproteolytic cleavage and activation of human acid ceramidase. J Biol Chem 283: 11253-9

Siskind LJ, Davoody A, Lewin N, Marshall S, Colombini M (2003) Enlargement and contracture of C2-ceramide channels. Biophys J 85: 1560-75

Siskind LJ, Kolesnick RN, Colombini M (2002) Ceramide channels increase the permeability of the mitochondrial outer membrane to small proteins. J Biol Chem 277: 26796-803

Siskind LJ, Kolesnick RN, Colombini M (2006) Ceramide forms channels in mitochondrial outer membranes at physiologically relevant concentrations. Mitochondrion 6: 118-25

Smith PK, Krohn RI, Hermanson GT, Mallia AK, Gartner FH, Provenzano MD, Fujimoto EK, Goeke NM, Olson BJ, Klenk DC (1985) Measurement of protein using bicinchoninic acid. Anal Biochem 150: 76-85

Stoffel W (1973) Chemistry and biochemistry of sphingosine bases. Chem Phys Lipids 11: 318-34

Stoffel W, Bister K (1974) Studies on the desaturation of sphinganine. Ceramide and sphingomyelin metabolism in the rat and in BHK 21 cells in tissue culture. Hoppe Seylers Z Physiol Chem 355: 911-23

Stoffel W, Melzner I (1980) Studies in vitro on the biosynthesis of ceramide and sphingomyelin. A reevaluation of proposed pathways. Hoppe Seylers Z Physiol Chem 361: 755-71

Stoffel W, Sticht G (1967) Metabolism of sphingosine bases, I. Degradation and incorporation of (3-14C)erythro-DL-dihydrosphingosine and (7-3H2)erythro-DL-sphingosine into sphingolipids of rat liver. Hoppe Seylers Z Physiol Chem 348: 941-3

Takeda S, Mitsutake S, Tsuji K, Igarashi Y (2006) Apoptosis occurs via the ceramide recycling pathway in human HaCaT keratinocytes. J Biochem 139: 255-62

Tani M, Iida H, Ito M (2003) O-glycosylation of mucin-like domain retains the neutral ceramidase on the plasma membranes as a type II integral membrane protein. J Biol Chem 278: 10523-30

Tsuboi K, Takezaki N, Ueda N (2007) The N-acylethanolamine-hydrolyzing acid amidase (NAAA). Chem Biodivers 4: 1914-25

Venkataraman K, Futerman AH (2001) Comparison of the metabolism of L-erythro- and L-threo-sphinganines and ceramides in cultured cells and in subcellular fractions. Biochim Biophys Acta 1530: 219-26

Wang G, Silva J, Dasgupta S, Bieberich E (2008) Long-chain ceramide is elevated in presenilin 1 (PS1M146V) mouse brain and induces apoptosis in PS1 astrocytes. Glia 56: 449-56

Watanabe M, Kitano T, Kondo T, Yabu T, Taguchi Y, Tashima M, Umehara H, Domae N, Uchiyama T, Okazaki T (2004) Increase of nuclear ceramide through caspase-3-dependent regulation of the "sphingomyelin cycle" in Fas-induced apoptosis. Cancer Res 64: 1000-7

Wendeler M, Hoernschemeyer J, Hoffmann D, Kolter T, Schwarzmann G, Sandhoff K (2004) Photoaffinity labelling of the human GM2-activator protein. Mechanistic insight into ganglioside GM2 degradation. Eur J Biochem 271: 614-27

Wendeler M, Werth N, Maier T, Schwarzmann G, Kolter T, Schoeniger M, Hoffmann D, Lemm T, Saenger W, Sandhoff K (2006) The enzyme-binding region of human GM2-activator protein. Febs J 273: 982-91

Wilkening G, Linke T, Sandhoff K (1998) Lysosomal degradation on vesicular membrane surfaces. Enhanced glucosylceramide degradation by lysosomal anionic lipids and activators. J Biol Chem 273: 30271-8

Xu X, Bittman R, Duportail G, Heissler D, Vilcheze C, London E (2001) Effect of the structure of natural sterols and sphingolipids on the formation of ordered sphingolipid/sterol domains (rafts). Comparison of cholesterol to plant, fungal, and disease-associated sterols and comparison of sphingomyelin, cerebrosides, and ceramide. J Biol Chem 276: 33540-6

Yoshimura Y, Okino N, Tani M, Ito M (2002) Molecular Cloning and Characterization of a Secretory Neutral Ceramidase of Drosophila melanogaster. J Biochem (Tokyo) 132: 229-36.

Yu C, Alterman M, Dobrowsky RT (2005) Ceramide displaces cholesterol from lipid rafts and decreases the association of the cholesterol binding protein caveolin-1. J Lipid Res 46: 1678-91

Yuan W, Qi X, Tsang P, Kang SJ, Illarionov PA, Besra GS, Gumperz J, Cresswell P (2007) Saposin B is the dominant saposin that facilitates

lipid binding to human CD1d molecules. Proc Natl Acad Sci U S A 104: 5551-6

Zeller CB, Marchase RB (1992) Gangliosides as modulators of cell function. Am J Physiol 262: C1341-55

Zhang Z, Mandal AK, Mital A, Popescu N, Zimonjic D, Moser A, Moser H, Mukherjee AB (2000) Human acid ceramidase gene: novel mutations in Farber disease. Mol Genet Metab 70: 301-9

7 Abbreviations

AcOH	acetic acid
BCA	Bicinchoninic Acid
BEVS	baculovirus expression vector system
BHK	baby hamster kidney
BMP	bis(monoacylglycero)phosphate
BSA	bovine serum albumin
CER	Ceramide
Cys	cysteine
DEAE	diethylaminoethyl
DMSO	Dimethylsulfoxide
DSG	Disuccinimidyl glutarate
DTT	dithiothreitol
EC	enzyme classification
EDTA	ethylendiamine
ER	endoplasmic retikulum
EtOH	ethanol
g	gravitational force
GSL	glycosphingolipid
h	hours
haCerase	human acid ceramidase
HPLC	high pressure liquid chromatography
IgG	Immunoglobulin G
k	kilo
MALDI	matrix assisted laser desorption ionization
MeOH	methanol
min	minutes
mg	milligram

mM	milli molar
MOI	Multiplicity of infection
μM	micro molar
MS	mass spectrometry
n	nano
NaAc	sodium acetate
NaCi	sodium citrate
NBT	nitrotetrazolium blue
nm	nano meter
NP-40	nonidet P 40
OPA	ortho-phthaldialdehyde
PAGE	polyacrylamide gel electrophoresis
PBS	phosphate buffered saline
PC	phosphatidylcholine
PCR	Polymerase chain reaction
PFA	paraformaldehyde
PFU	plaque-forming units
PG	phosphatidylglycerol
PI	phosphatidylinositol
pI	isoelectric point
PMSF	phenylmethylsulfonylfluoride
PVDF	poly(vinylden)diflouride
RT	room temperature
SAP	sphingolipid activator protein
SDS	sodium dodecylsulfate
SEAP	secretory alkaline phosphatase
Sf	spodoptera frugiperda
Tev protease	Tobacco Etch Virus protease
TFA	trifluoroacetic acid

Tricine	N-[tris(hydroxymethyl)methyl]glycin
Tris	tris(hydroxymethyl)aminomethane
v/v	volume per volume
w/v	weight per volume

8 Supplements

Tryptic peptides with at least 3 amino acid residues	$[M+H]^+$ calculated (Da)	$[M+H]^+$ measured (Da)
T1 (-)QHAPPWTED**C**R	1339.59	–
T3 STYPPSGPTYR	1225.59	1225.46
T4 GAVPWYTINLDLPPYK	1846.97	1847.60
T6 WHELMLDK	1071.53	1071.67
T7 APMLK	559.33	–
T8 VIVNSLK	772.49	–
T9 NMINTFVPSGK	1207.61	1207.71
T10 VMQVVDEK	947.49	–
T11 LPGLLGNFPGPFEEEMK	1874.94	1875.59
T12 GIAAVTDIPLGEIISFNIFYELFTI(-)	2756.48	2756.82
T13 (-)**C**TSIVAEDK	964.45	–
T15 GHLIHGR	789.45	789.54
T16 NMDFGVFLGWNIN**N**DTWVITEQLKPLTVNLDFQR	4038.02	–
T17 NNK	375.20	–
T18 TVFK	494.30	–
T19 ASSFAGYVGMLTGFKPGLFSLTLNER	2763.42	2764.06
T20 FSINGGYLGILEWILGK	1880.03	1880.62
T22 DAMWIGFLTR	1209.61	1209.56
T23 TVLE**N**STSYEEAK	1470.70	–
T24 NLLTK	588.37	–
T25 ILAPAYFILGG**N**QSGEG**C**VITR	2279.19	-
T26 ESLDVYELDAK	1281.62	–
T30 QGR	360.20	–
T31 WYVVQTNYDR	1343.64	1342.56
T33 HPFFLDDR	1046.51	1046.55
T35 TPAK	416.25	–
T36 M**C**LNR	636.30	–
T37 TSQE**N**ISFETMYDVLSTKPVLNK	2644.32	2644.62
T38 LTVYTTLIDVTK	1366.78	1366.54
T39 GQFETYLR	1013.51	1013.46
T40 D**C**PDP**C**IGW	1005.38	–

Table of MALDi and ESI fragments of human acid ceramidase (Taken from Schulze et al, 2007)